Psychological Review
2016, Vol. 123, No. 3, 305–323

0033-295X/16/$12.00 http://dx.doi.org/10.1037/rev0000029

# Affordance-Based Perception-Action Dynamics: A Model of Visually Guided Braking

Henry S. Harrison, Michael T. Turvey, and Till D. Frank
University of Connecticut

Behavioral dynamics is a framework for understanding adaptive behavior as arising from the self-organizing interaction between animal and environment. The methods of nonlinear dynamics provide a language for describing behavior that is both stable and flexible. Behavioral dynamics has been criticized for ignoring the animal's sensitivity to its own capabilities, leading to the development of an alternative framework: affordance-based control. Although it is theoretically sound and empirically motivated, affordance-based control has resisted characterization in terms of nonlinear dynamics. Here, we provide a dynamical description of affordance-based control, extending behavioral dynamics to meet its criticisms. We propose a general modeling strategy consistent with both theories. We use visually guided braking as a representative behavior and construct a novel dynamical model. This model demonstrates the possibility of understanding visually guided action as respecting the limits of the actor's capabilities, while still being guided by informational variables associated with desired states of affairs. In addition to such "hard" constraints on behavior, our framework allows for the influence of "soft" constraints such as preference and comfort, opening a new area of inquiry in perception-action dynamics.

*Keywords:* perception and action, perceptual-motor control, dynamical systems, self-organization, driving



Adaptive behavior is characterized by both stability and flexibility, robust to both perturbation and changing circumstance. We can understand these patterns of behavior not as imposed by prior organization in the body or brain but rather as self-organizing from the interaction between animal and environment (Warren, 2006). This perspective identifies perception and action as the foundation for understanding the behavior of humans and other animals. Of primary interest is the coordination of action with respect to perception.

Much psychological research and theory has been directed at elucidating the nature of this animal–environment coupling. Vision has been particularly scrutinized (see, e.g., Turvey, 1977), perhaps because structured reflected light provides an important source of information for the Kingdom Animalia (Margulis & Schwartz, 1988). Inquiry into visually guided action reveals principles of perception and action that apply beyond the particular behavior and species under examination. Furthermore, the same principles apply to action guided by means other than vision, as research on echolocation in bats has indicated (Lee, Simmons, Saillant, & Bouffard, 1995; Lee, van der Weel, Hitchcock, Matejowsky, & Pettigrew, 1992). In this essay, we will focus on the task of stopping a vehicle by braking, with the understanding that the knowledge gained from this inquiry is applicable to the ubiquitous behavior of closing gaps in a controlled manner, to visually guided action in general, and to perception-action as a whole.

General proposals for understanding the regulation of movement with respect to the environment can be grouped into two fundamentally different conceptual approaches. One strategy is to posit internal representations of body and environment dynamics that are called upon to predict the consequences of movement and plan accordingly (e.g., Kawato, 1999; Wolpert, 1997). Gibson (1958, 1979) pioneered an alternative approach, proposing that optical information can guide action directly, without the need for mediation by internal models or other representations. This is possible because movement relative to the layout of surfaces generates *optic flow*, continuous transformations of the optic array at the point of observation. Some properties of this flow fall into a one-to-one relationship with behaviorally relevant states of the animal–environment system. Such properties are invariant, higher order relations within the changing optic array. The upshot is that visually guided, goal-directed action can be accomplished by stabilizing an optic-flow variable that specifies the desired animal–environment relationship. Similarly, negative outcomes can be prevented by avoiding invariants that specify undesired states (e.g., collisions). This approach has been empirically validated for a number of perception-action behaviors. Notable examples include steering (Fajen & Warren, 2004; Warren & Fajen, 2004, 2008), braking (Bardy & Warren, 1997; Lee, 1976), and catching a fly ball (Chapman, 1968; Fink, Foo, & Warren, 2009; McBeath, Shaffer, & Kaiser, 1995; P. McLeod, Reed, & Dienes, 2006; Michaels & Oudejans, 1992; Michaels & Zaal, 2002). This approach has been termed *information-based control*, to distinguish

This article was published Online First February 15, 2016.

Henry S. Harrison, Michael T. Turvey, and Till D. Frank, Center for the Ecological Study of Perception and Action, Department of Psychological Sciences, University of Connecticut.

Correspondence concerning this article should be addressed to Henry S. Harrison, Center for the Ecological Study of Perception and Action, Department of Psychological Sciences, University of Connecticut, 406 Babbidge Road, Unit 1020, Storrs, CT 06269-1020. E-mail: henry.schafer.harrison@gmail.com

it from model-based control as well as *affordance-based control* (Fajen, 2007a), which we will describe later.

Vehicular braking in particular has been a paradigmatic behavior for studying visually guided action, inspiring the first thorough, mathematical demonstration that optic flow contains information sufficient for the control of action (Lee, 1976). Braking as a behavior is not some incidental side effect of human artifice but rather represents a general class of actions. Across the animal kingdom, closing gaps in a controlled manner is at least as universal as locomotion (Lee, 1998, 2014; Pepping & Grealy, 2007). A dragonfly chasing a mosquito, a horse leaping over a fence, a batter hitting a baseball, and the fielder catching it all must control the nature of the resulting collision. We can classify these actions based on the desired momentum transfer at the point of contact (Kugler, Turvey, Carello, & Shaw, 1985). A hard collision results in some transfer of momentum, whereas a soft collision does not. This distinction is crucial. A tennis player must transfer momentum from the racket to the ball. The appropriate magnitude and direction of this transfer is integral to the action's success. A hummingbird landing on a feeder, on the other hand, must avoid a transfer of momentum—too much velocity at the point of contact and the bird will fall forward off the perch.

The braking problem, as it has been studied since Lee (1976), is a proxy for the soft-contact class of controlled collisions. When studied using a driving simulator (Yilmaz & Warren, 1995), the experimental task is to come to a stop "as close as possible" to an obstacle. This is not precisely the same task as an automobile driver encounters, coming to a stop at any point in front of the obstacle. Although this distinction must be kept in mind, the experimental version of the task is similar to the general problem of soft collisions found across the animal kingdom. As such, it has provided an avenue for understanding visually guided action in general. Two questions lie at the core of the braking problem:

1. What visual information is used to regulate braking?

2. How is this information used? In other words, how does visual information constrain the driver's actions?

Proposing an answer to these questions, Lee (1976) identified the optical variable tau ($\tau$), the ratio of an object's optical size to its rate of optical expansion, as an invariant. Specifically,

$$\tau = \theta/\dot{\theta} = -x/v, \tag{1}$$

where $\theta$ is the visual angle subtended by the obstacle, $x \leq 0$ is the position of the observer relative to the obstacle at $x = 0$, $v = \dot{x}$ is the observer's velocity, and dot notation indicates rate of change (i.e., $\dot{u} = du/dt$). Importantly, $-x/v$ is equal to the time remaining until a collision if the current speed is maintained. Thus, Equation 1 demonstrates a higher order optical variable that specifies a behaviorally relevant property of the organism–environment system, namely, time-to-contact.

The optical variable $\tau$ has inspired a variety of experimental, observational, and theoretical studies. Early experiments established that observers use $\tau$ to estimate time-to-contact (Cavallo & Laurent, 1988; Kaiser & Mowafy, 1993; R. W. McLeod & Ross, 1983; Todd, 1981). In addition to these explicit judgment and estimation tasks, $\tau$ was implicated in the timing of movement initiation. Famously, observations of gannets diving into the ocean appeared consistent with the hypothesis that the birds use $\tau$ to time their adjustment of the wings just prior to hitting the water (Lee & Reddish, 1981). Other early findings supported a role for $\tau$ in human participants' timing of interceptive movements (Bootsma & van Wieringen, 1990, 1988; Lee, Young, Reddish, Lough, & Clayton, 1983) as well as the regulation of gait over uneven terrain (Lee, Lishman, & Thomson, 1982; Warren, Young, & Lee, 1986). However, these results were called into question (Wann, 1996), as was the distinction between movement initiation and movement execution (Bootsma, Fayt, Zaal, & Laurent, 1997).

In the realm of continuous control, Lee (1976) originally demonstrated that tau-dot ($\dot{\tau}$), the rate of change of $\tau$, specifies the sufficiency of the current rate of deceleration. A soft collision is possible when $\dot{\tau}$ is maintained within $-1 < \dot{\tau} < 0$. However, in the region of $-1 < \dot{\tau} < -0.5$, deceleration must progressively increase and, eventually, infinite deceleration is required to come to a stop. For this reason, to close a gap without transfer of momentum, $-0.5 \leq \dot{\tau} < 0$ must be maintained. In particular, when $\dot{\tau}$ is held constant at $-0.5$, deceleration will be constant and, thus, braking force will be minimized. The classic constant-$\dot{\tau}$ strategy, then, is to hold $\dot{\tau}$ constant at some margin value $\dot{\tau}_m = -0.5$. Thus, the constant-$\dot{\tau}$ strategy holds that drivers increase deceleration when $\dot{\tau} < -0.5$ and decrease deceleration when $\dot{\tau} > -0.5$.

In short, the optical variable $\dot{\tau}$ provides informational support for the perception of the severity of an upcoming collision. Similarly, control of $\dot{\tau}$ allows an actor to control the severity of an upcoming collision. Furthermore, $\dot{\tau}$ has the advantage of being a dimensionless variable. This means that its properties are independent of the units used to measure quantities such as time or length. Detection of $\dot{\tau}$, and its use in the guidance of action, does not require a mental clock or ruler or any other metric (Runeson, 1977).

The constant-$\dot{\tau}$ strategy was supported by an estimation task in which participants judged the severity of an upcoming collision (Kim, Turvey, & Carello, 1993). Observations of landing hummingbirds (Lee, Reddish, & Rand, 1991) and pigeons (Lee, Davies, Green, & van der Weel, 1993) are also consistent with the strategy, as are deceleration profiles from human participants in a virtual braking task (Yilmaz & Warren, 1995).

However, Bardy and Warren (1997) note that these results are consistent with a variety of control strategies. Observed values of $\dot{\tau}$ could be the effect, rather than the cause, of controlled deceleration. Anticipating the concerns of Fajen (2007a) that we will discuss shortly, Bardy and Warren (1997) also note that the dynamics of the controller (e.g., the design of the brake) must also be taken into account. Complicating matters further, it is now clear that information other than $\dot{\tau}$ is used when available (Andersen & Sauer, 2004; Fajen, 2005b; Rock & Harris, 2006). Taken together, the body of evidence suggests that $\dot{\tau}$ is an important, but not necessarily exclusive, optical variable for controlled deceleration. Additionally, the simplicity of the constant-$\dot{\tau}$ strategy belies the difficulty in constructing a control strategy based on the optical variable.

Fajen (2005a, 2005c) has developed a conceptual critique of the constant-$\dot{\tau}$ strategy. The original $\dot{\tau}$ hypothesis in its simplicity overlooks an important aspect of real-world action: physical limitations. The ability to decelerate is always finite. Within this limit, it may not be possible to enact the constant-$\dot{\tau}$ strategy. The only guarantor of success is that the required deceleration (that which produces $\dot{\tau} = \dot{\tau}_m = -0.5$) remains within the bounds of the maximum achievable deceleration. This distinction is subtle. Whereas the original contribution of Lee (1976) was to demonstrate that a sufficient condition for coming to a stop without colliding is the generation of the invariant $\dot{\tau} = -0.5$, Fajen (2005a, 2005c) suggests an extension: a *necessary* and sufficient condition for braking is that generation of the invariant $\dot{\tau} = -0.5$ *remains possible*. Framing the control problem in terms of possibilities allows a description of the *necessary* conditions for successful action, thus generalizing any number of specific strategies, each of which describes a *sufficient* condition for successful action. Applied to visually guided action more broadly, Fajen (2007a) calls this approach *affordance-based control*. Affordances, possibilities for action, provide a description of the environment at the level most relevant to the prospective control fundamental to the Kingdom Animalia (Gibson, 1979; Turvey, 1992).

Affordance-based control has a number of implications for understanding visually guided action. For one, it implies that awareness of one's limits is required for successful action. Evidence that drivers take into account their maximum deceleration comes from a series of experiments in which participants adjusted their behavior following abrupt changes in brake dynamics (Fajen, 2005c, 2007b). A second implication of affordance-based control stems from the fact that it expands the set of trajectories considered successful. The original $\dot{\tau}$ strategy admits only one correct state at any given time: that which generates the invariant $\dot{\tau} = -0.5$. Fajen's revision (2005a, 2005c), however, invites researchers to consider all the routes a driver might take to reach a complete stop: sometimes gently, sometimes abruptly. Thus, affordance-based control provides a framework for investigating the factors that cause these variations, such as risk aversion and aggressive driving. Finally, and perhaps most importantly, affordance-based control bridges a theoretical divide between two major prongs of perception-action research. On one side, there is a rich body of work focused on the perception of affordances (e.g., Fitzpatrick, Carello, Schmidt, & Corey, 1994; Lopresti-Goodman, Turvey, & Frank, 2011, 2013; Mark, 1987; Regia-Corte & Wagman, 2008; Warren, 1984; Wraga, 1999). On the other, there is research on the continuous control of visually guided action (e.g., Jacobs & Michaels, 2006; Michaels & Zaal, 2002; Peper, Bootsma, Mestre, & Bakker, 1994; Saltzman & Kelso, 1987; Warren, 1988, 2006; Warren & Fajen, 2004; Warren, Kay, Zosh, Duchon, & Sahuc, 2001). Despite shared theoretical commitments (e.g., Gibson, 1979), these research programs have proceeded more or less independently. Fajen's (2007a) proposal begins to close this gap.

Information-based control strategies that are based on nulling the error in some optical variable, such as the constant-$\dot{\tau}$ strategy, are naturally modeled in a dynamical framework (Warren, 1988, 2006). This has undoubtedly contributed to their success. However, applying these advances to affordance-based control remains problematic, as describing control in terms of possibility rather than actuality seems to render modeling impossible. If the control strategy indicates a range of allowable actions rather than a single required action, how can a model predict individual trajectories? The first step must be the identification of the factors responsible for variation among realizations of the same affordance.

To this end, we have previously mentioned somewhat vague psychological factors such as aggression and risk aversion. Fajen (2005a) terms these types of influences "styles of control." Whereas under information-based control radically different trajectories appear to be products of different control strategies, affordance-based control accommodates these variations under a single control strategy. Drivers using the same strategy (keep required deceleration from surpassing maximum deceleration) may vary in the significance placed on various costs (e.g., approach time, margin of safety). From a modeling perspective, this suggests the minimization of cost functions to collapse possible outcomes to actual outcomes and thereby model individual trajectories. The minimization of cost functions is the cornerstone of the optimal control approach (Todorov, 2004; Todorov & Jordan, 2002). These models typically require the explicit prediction of future states. For example, determining the value of the "optimal cost-to-go" function posited by some optimal control models requires the consideration of all possible future states (Todorov, 2004). Optimality control is thus a variant of the model-based approach, and is therefore fundamentally incompatible with shared theoretical principles of information-based (Warren, 2006) and affordance-based (Fajen, 2007a) control. However, an accommodation may be possible. Perhaps the optimal cost-to-go function could be learned, rather than computed, in a manner compatible with an ecological approach to learning (e.g., Jacobs & Michaels, 2007).

Alternatively, it may be possible to understand styles of control without invoking cost functions. Fajen (2005c, 2007a) uses the terminology "soft constraints" to refer to situation-specific factors that influence the emergence of specific trajectories (cf. Kugler & Turvey, 1987). In contrast, the action boundary separating possible from impossible actions and defining the affordance-based control strategy defines a hard constraint: It determines what constitutes success, and therefore cannot be violated. Soft constraints, on the other hand, are mere preferences that shape the resulting trajectory but do not define success or failure conditions. Perhaps the only difference between hard and soft constraints is whether or not violations are tolerated. The challenge, then, is to identify a mathematical distinction that formalizes this intuition.

A focus on constraints clarifies the distinction between information- and affordance-based control. The hard constraint for information-based models is typically a sufficient condition for success. Affordance-based control, on the other hand, defines hard constraints in terms of necessary and sufficient conditions for success (or conversely, in terms of the action's failure conditions). In doing so, it invites the study of soft constraints, difficult to include in an information-based control framework. It is important to keep in mind, however, that affordance-based control strategies must still be grounded in the information available to the organism (Fajen, 2007a). Thus, affordance-based control is not a departure from the fundamental principle that action is regulated by information, in the sense of specification. Rather, it is a call for researchers to consider additional sources of information: those that specify the perceiver's action boundaries. For these reasons, framing the issue as a choice between two competing approaches, information- and affordance-based, is misleading. A more accurate formulation would consider affordance-based control to be an extension of information-based control. Affordance-based control extends information-based control, inviting us to consider not only the information associated with *actual* outcomes but also the information associated with *possible* outcomes. This expansion of control theory from the realm of actuality to the realm of possibility coincides with the role of natural law. Laws define what is possible, whereas circumstances determine what actually occurs. In general, "laws + circumstances = actuality" (Park & Turvey, 2008, p. 3). Thus, we may identify hard constraints with natural laws, and soft constraints with circumstances. In this light, affordance-based control promises a theory of action aligned with ecological theory, as a result of not only the emphasis on affordances but also the commitment to a law-based understanding of behavior.

To that end, we will propose here a model of visually guided braking that extends existing information-based models (Lee, 1976; Warren, 2006) in order to satisfy the principles of affordance-based control (Fajen, 2007a). First, we will describe existing models of visually guided braking and, in so doing, introduce the formalism of behavioral dynamics (Warren, 2006), closely associated with information-based control. We will develop a vocabulary for understanding information-based control models, which we will bring to bear on the phenomenology of affordance-based control.

## Existing Models of Visually Guided Braking

Control strategies in the information-based approach are typically modeled as control laws (Warren, 1988, 2006). In the formalism of behavioral dynamics (Warren, 2006), laws of control mirror the laws of physics. The laws of physics describe how the state of the environment changes as a function of the current state of the environment as well as external forces. Similarly, control laws describe how the state of the organism changes as a function of its current state as well as available information.

Formally, an acting organism, or "actor," can be described with a system of first-order differential equations (Warren, 2006),

$$\dot{\boldsymbol{\alpha}} = \boldsymbol{\Psi}(\boldsymbol{\alpha}, \mathbf{i}), \tag{2}$$

where $\alpha$ is a vector of the actor's state variables,[1] $\mathbf{i}$ is a vector of informational variables, and $\boldsymbol{\Psi}$ is a control law. The role of the control law then becomes one of modulating the system's ongoing dynamics on the basis of available optical information $\mathbf{i}$.

### The $\dot{\tau}$ Control Law

As a demonstration of his approach to behavioral dynamics, Warren (2006) developed a control law for braking based on Lee's (1976) original $\dot{\tau}$ strategy. The control law describes adjustments in brake-pedal position $z$ as

$$\Delta z = b_{\text{pedal}}(\dot{\tau}_{\text{m}} - \dot{\tau}) + \epsilon, \tag{3}$$

where $z$ is brake position, $b_{\text{pedal}} > 0$ is a stiffness parameter determining the speed of pedal adjustments, and $\varepsilon$ is a noise term. Thus, when $\dot{\tau} = \dot{\tau}_{\text{m}}$,[2] the current braking strength is maintained; otherwise, the magnitude of the brake adjustment is proportional to the deviation of $\dot{\tau}$ from the desired margin value. Equation 3 meets the information-based standard because all its variables fall into the following categories: action variables ($z$), informational variables ($\dot{\tau}$), free parameters ($b_{\text{pedal}}$), and noise ($\varepsilon$). It assumes no knowledge of the state of the system that is not continuously available in optic-flow patterns.

Implicit in Equation 3 is the assumption that $\tau$ and brake position $z$ are coupled, though the connection between these variables has not yet been formalized. We already have a relation between $\tau$ and displacement, Equation 1; for simplicity, we assume a linear relationship between brake position and acceleration. We will also restate the control law as a system of first-order differential equations, to match the formalism of Equation 2. Then, a complete description of the $\dot{\tau}$ control law as a system of first-order differential equations is

$$\begin{aligned} \dot{\alpha}_1 &= \dot{x} = \Psi_1(\alpha) = v \\ \dot{\alpha}_2 &= \dot{v} = \Psi_2(\alpha) = a \\ \dot{\alpha}_3 &= \dot{a} = \Psi_3(\alpha) = -b_{\dot{\tau}}(\dot{\tau}_{\text{m}} - \dot{\tau}), \end{aligned} \tag{4}$$

where $\alpha_1 = x \leq 0$ is the position of the actor relative to the obstacle at $x = 0$, $\alpha_2 = v$ is the actor's velocity, $\alpha_3 = a \leq 0$ is the actor's acceleration,[3] $b_{\dot{\tau}} > 0$ is a stiffness parameter determining the speed of $\dot{\tau}$ adjustments, and $\dot{\tau}_{\text{m}} = -0.5$ is the target margin value of $\dot{\tau}$.

We assume, for simplicity, that the informational variables $\mathbf{i}$ are a function of the state vector $\boldsymbol{\alpha}$, and therefore $\mathbf{i}$ need not be a distinct parameter of $\boldsymbol{\Psi}$. For example, per Equation 1, the informational variable $\dot{\tau}$ is a function of $\alpha_1 = x$ and $\alpha_2 = v$. This questions the need in Equation 2 to specify informational variables separately from the state vector. The most compelling reason to do so is theoretical: Per the principles of information-based control, variables used by the actor must be available optically (or acoustically, mechanically, etc.). The distinction between $\mathbf{i}$ and $\boldsymbol{\alpha}$ reminds the theorist that whereas the system's intrinsic dynamics are a function of the state vector $\boldsymbol{\alpha}$, any modulation of these dynamics reflecting visually guided action can only be a function of optical variables $\mathbf{i}$. Practically, however, a mapping $\mathbf{i} = \boldsymbol{\lambda}(\boldsymbol{\alpha})$ must exist, reflecting the laws of ecological optics, haptics, and so forth (Warren, 2006), and therefore the modeler can absorb this function $\boldsymbol{\lambda}$ into the general dynamics $\boldsymbol{\Psi}$. The only caveat is to ensure that the resulting model does not violate this principle of informational availability; this is a concern we will address repeatedly. As an initial sketch, of the three elements of the vector equation Equation 4 we classify $\dot{x} = \Psi_1(\boldsymbol{\alpha})$ and $\dot{v} = \Psi_2(\boldsymbol{\alpha})$ as reflecting intrinsic dynamics (with $\dot{a} = 0$), whereas $\dot{a} = \Psi_3(\boldsymbol{\alpha})$ reflects their modulation on the basis of available visual information.

We also note, briefly, that the formalism of Warren (2006) also separates state variables into actor variables $\boldsymbol{\alpha}$ and environment variables $\mathbf{e}$; for him, $\boldsymbol{\lambda}$ is a function of $\mathbf{e}$ rather than $\boldsymbol{\alpha}$. We question this choice, noting that information is a function of the actor–environment system (e.g., $\dot{\tau}$) rather than solely the

[1] Although Warren (2006) uses $\mathbf{a}$ to denote the vector of action variables, we use $\boldsymbol{\alpha}$ to prevent confusion with acceleration $a$.

[2] Yilmaz and Warren (1995) determined an empirical margin value $\dot{\tau}_{\text{m}} = -0.52$, although for simplicity we assume $\dot{\tau}_{\text{m}} = -0.5$ in our analyses.

[3] For clarity, we occasionally refer to $a$ as *deceleration*; because we specify the constraint $a \leq 0$, we use these terms interchangeably with the same meaning.

environment. By referring to $\boldsymbol{\alpha}$ as state variables rather than actor variables, we avoid the messy and theoretically suspect task of labeling each state variable as belonging to either the actor or the environment. We believe that this edit of the behavioral dynamics formalism is a minor one and does not impact its practical utility or theoretical relevance. However, we leave the important task of working out the remaining details in light of this change for later investigation.

Returning now to Equation 4, simulations will be aided by deriving a formula for $\dot{\tau}$ in terms of only the state variables. By applying the quotient rule to Equation 1, we arrive at

$$\dot{\tau}(\boldsymbol{\alpha}) = \frac{xa}{v^2} - 1. \tag{5}$$

For illustration purposes, solutions of Equation 4 were estimated numerically. A relaxation was observed, stabilizing at $\dot{\tau} = \dot{\tau}_m$, resulting in a constant deceleration until $x = v = 0$ is approached. One such trajectory is shown in Figure 1.

## The Deceleration-Error Model

Fajen (2005a; see also Yilmaz & Warren, 1995, Strategy 3) proposes an alternative control law for braking, the *deceleration-error model*. In this model, rather than null the difference between $\dot{\tau}$ and $\dot{\tau}_m$, the actor nulls the difference between deceleration $a$ and "ideal" deceleration $a_{\text{ideal}}$, where $a_{\text{ideal}}$ is the deceleration that would produce $\dot{\tau} = \dot{\tau}_m$. This can be derived from Equation 5 as

$$a_{\text{ideal}} = \frac{v^2}{2x}. \tag{6}$$

The initial challenge for the deceleration-error model is to demonstrate that $a_{\text{ideal}}$ is available to the actor. To this end, we note two optical variables that specify actor speed $v$. Global optic flow rate (GOFR), the rate of optical motion of texture elements, is proportional to $v$ when eyeheight is constant. Alternatively, edge rate (ER), the rate at which texture elements pass a fixed optical reference point, is proportional to $v$ as long as texture density is constant (Larish & Flach, 1990). Therefore, along with Equation 1, we can derive $a_{\text{ideal}}$ in terms of only optical variables (Fajen, 2005a)

$$a_{\text{ideal}} = -k\frac{\text{GOFR}}{2\tau} = -k\frac{\text{ER}}{2\tau}, \tag{7}$$

where $k$ is some constant.

Actors are indeed sensitive to changes in GOFR and ER in a braking task, a result which cannot be explained by the $\dot{\tau}$ strategy (Fajen, 2005a). Of these variables, Fajen (2005a) also found that both GOFR and ER contribute to braking performance, although the contribution of GOFR was significantly greater. It is also possible that the relative contribution of these variables depends on context. For example, during typical locomotion, participants steer using optic flow; however, participants will rely on egocentric heading direction in an environment with limited optical structure (Warren et al., 2001). A similar situation may hold between GOFR and ER.

The deceleration-error model also requires that there is available information about current deceleration $a$. Possibilities include that deceleration is detected by the vestibular system (Harris et al., 2002), and that the relevant information is generated by the resistance and position of the brake and picked up by haptic extero- and proprioperception (Fajen, 2005a).

A full description of the deceleration-error control law is

$$\begin{aligned}
\dot{\alpha}_1 &= \dot{x} = \Psi_1(\boldsymbol{\alpha}) = v\\
\dot{\alpha}_2 &= \dot{v} = \Psi_2(\boldsymbol{\alpha}) = a\\
\dot{\alpha}_3 &= \dot{a} = \Psi_3(\boldsymbol{\alpha}) = -b'_a(a - a_{\text{ideal}}),
\end{aligned} \tag{8}$$

where, similar to previous $b$ parameters, $b'_a > 0$ is a stiffness parameter (the prime is to distinguish this parameter from a derived parameter $b_a$ which we will introduce later), this time determining the speed of deceleration adjustments. A simulated trajectory of Equation 8 is shown in Figure 1, alongside a simulated trajectory of Equation 4, the $\dot{\tau}$ control law. As $a_{\text{ideal}}$ is defined as the deceleration that produces $\dot{\tau} = -0.5$, the behavior of the deceleration-error model is similar to that of the $\dot{\tau}$ model: Relaxation to $\dot{\tau} = \dot{\tau}_m = -0.5$ is observed, followed by a constant rate of deceleration for the duration of the simulation.

## Fixed Points and Nullclines

In proposing a control law of steering during locomotion, Fajen and Warren (2003) analyzed cross-sections of state space following a simulated trajectory. This provides an intuitive perspective on dynamical systems that is integral to Warren's (2006) presentation of the behavioral dynamics framework. The steering dynamics model is formalized as a four-dimensional system comprising the actor's position ($x$, $z$), heading $\phi$, and turning rate $\dot{\phi}$ (Fajen & Warren, 2003). Fajen and Warren (2003) plot vector fields of $\ddot{\phi}$ against $\dot{\phi}$, holding $x$ and $z$ constant, in four different locations. This allows them to identify "attractors" and "repellers" of heading. However, these are technically not fixed points in the context of the entire dynamical system, as some rates of change remain nonzero (specifically, $\dot{x}$ and $\dot{z}$). Rather, these "fixed points" exist only transiently, in cross-sections of state space. In more formal terms, these are points that lie on nullclines, locations in state space at which the rate of change of one or more state variables is zero. The technique of examining high-dimensional state spaces with two-dimensional cross-sections allows Fajen and Warren to ignore the state variables with nonzero rates of change, $x$ and $z$. Although their model has no true fixed points, Fajen and Warren illustrate its behavior by referring to changes in the layout of attractors and repellers as the actor traverses ($x$, $z$) cross-sections of state space. Mathematically speaking, these points are not true attractors and repellers, but rather the locations where the current ($x$, $z$) cross-section intersects a nullcline. Nullclines have some, but not all, of the properties of fixed points. A point on a nullcline can be attractive or repellent, and their topology is of primary interest. Therefore, although Fajen and Warren were technically incorrect to refer to attractors and repellers, their cross-sectional analysis nonetheless yields important insights. For clarity, we will refer to the intersections between nullclines and state-space cross-sections as *pseudo*attractors and *pseudo*repellers.

We performed a similar analysis of the deceleration-error model. First, we note that, like with the steering-dynamics model, a rigorous fixed-point analysis is not helpful: When the actor reaches $x = 0$, he is still decelerating, and so a true fixed point is not reached. Appendix A provides a more detailed description of this issue. The key point is that analyzing nullclines and pseudo-

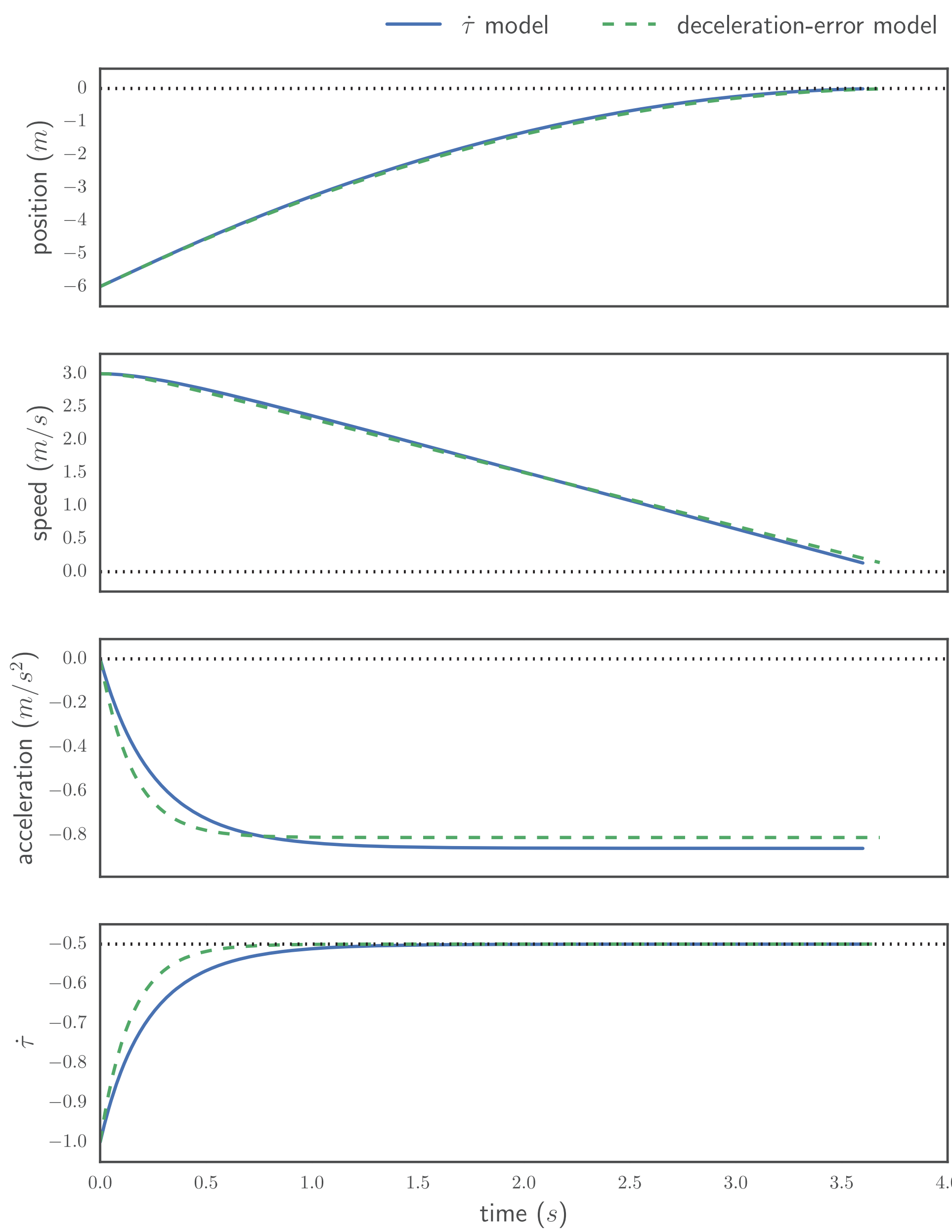


*Figure 1.* Solutions of Equation 4 ($\dot{\tau}$ control law) and Equation 8 (deceleration-error control law), with $b_{\dot{\tau}} = 7\text{m/s}^3$ for the former and $b'_a = 7\text{s}^{-1}$ for the latter, $\dot{\tau}_m = -0.5$, and initial conditions of $x = -6$ m, $v = 3$ m/s, and $a = 0$ m/s$^2$, estimated using the lsoda solver in the FORTRAN library odepack (Hindmarsh, 1983). See the online article for the color version of this figure.

attractors will be of more use than a traditional fixed-point analysis.

Three vector fields, of ($v$, $a$) cross-sections with decreasing displacement, are plotted in Figure 2. Where the arrows point up, the deceleration-error control law predicts increased deceleration, and where the arrows point down, it predicts decreased deceleration. Moreover, at $a = a_{\text{ideal}}$, there is a nullcline where $\dot{a} = 0$. This defines a two-dimensional surface in the three-dimensional state space; its intersection with a given ($v$, $a$) cross-section yields a curve. Accordingly, one way to understand the deceleration-error model, following the technique of Fajen and Warren (2003), is that for any distance from the obstacle, there is a pseudoattractor at $a = a_{\text{ideal}}$. As the actor moves toward the obstacle, the pseudoattractor shifts according to the incoming information (unless $a_{\text{ideal}}$ has already been reached, in which case it remains stationary). The dynamics here are relatively simple; at no point is a qualitative change observed in the cross-sectional vector fields. In the absence of a qualitative change, or bifurcation, the two ways in which dynamics may evolve in a cross-sectional analysis are (a) change in the location of the pseudoattractor, and (b) change in the strength of the pseudoattractor.

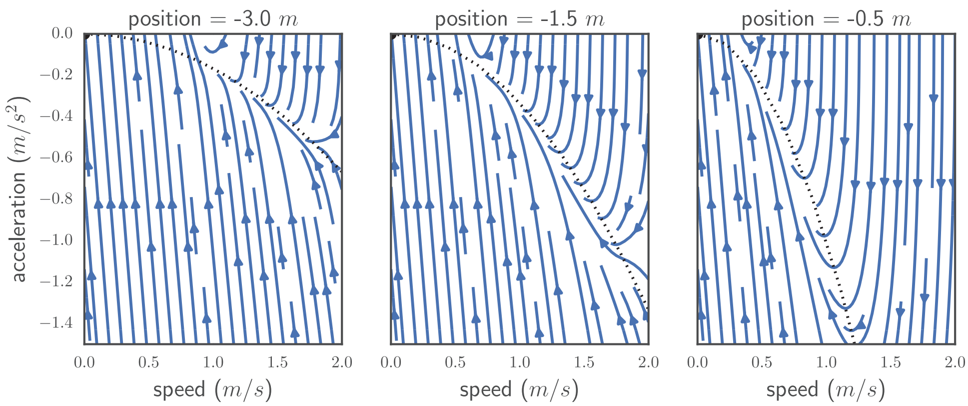


*Figure 2.* Vector fields of Equation 8, the deceleration-error model, at three cross-sections of state space with fixed postion $x$. The arrows show the rates of change of deceleration (vertical component) and velocity (horizontal component). The dotted lines show ideal deceleration, the intersections of the $\dot{a} = 0$ nullcline with each fixed-$x$ cross-section. See the online article for the color version of this figure.



Change in the location of the pseudoattractor is explicit in both Equations 4 and 8. As the nullcline is given by $\dot{a} = 0$, the expressions $\dot{\tau}_m - \dot{\tau}$ and $a - a_{\text{ideal}}$, respectively, neatly define the set of all pseudoattractor locations (i.e., the $\dot{a} = 0$ nullcline). In other words, the pseudoattractor locations in both equations are explicitly determined by the expression within the parentheses. Although these expressions are not equivalent, they are equal to zero at the same values of $x$, $v$, and $a$. Thus, these models have the same $\dot{a} = 0$ nullcline, defining the same surface in state space. To reflect the importance of this nullcline to our analysis (compared with the $\dot{x} = 0$ and $\dot{v} = 0$ nullclines), we will refer to it as the system's *attractive manifold*. The fact that the two control laws we have examined behave so similarly, as observed in Figure 1, can then be attributed to the fact that both systems have the same attractive manifold.

Thus, the only difference between the $\dot{\tau}$ model and the deceleration-error model is with respect to the *strength* of the pseudoattractor at each point in state space. Both models explicitly define the attractive manifold, the location of the pseudoattractor, but the strength of the pseudoattractor is given little attention. In these models, it is simply the distance from the pseudoattractor (e.g., the value of the parenthetical expression) multiplied by a stiffness parameter $b$.

The stiffness, or pseudoattractor strength, is therefore an opportunity to further modulate the behavioral dynamics on the basis of incoming information. Allowing stiffness, and therefore pseudoattractor strength, to vary systematically is not a novel strategy. Indeed, the previously mentioned steering model (Fajen & Warren, 2003, 2007) uses this technique to make the influence of goals and obstacles fade away with distance. This is the opening we will follow, in order to model affordance-based control of braking. We will leave the pseudoattractor location intact, but modify its strength to reflect the "urgency" of braking at any given moment. If this can be accomplished without introducing any variables not available to the actor, the resulting model will remain faithful to the principles of information-based control.

Although there is evidence favoring the deceleration-error model over the $\dot{\tau}$ model, neither model can explain observed sensitivity to the braking action boundary (Fajen, 2005a). These models are based on information about the sufficiency of current deceleration, but not its necessity. When braking is not urgent, stabilizing $\dot{\tau} = -0.5$ is unnecessary and information about sufficiency may be ignored in favor of soft constraints on behavior. In the case of emergency braking, information about the action boundary, maximum deceleration, would allow actors to perceive the possibility of collision avoidance, rather than (or in addition to) the sufficiency of the current course of action.

Fajen (2005a) emphasizes that both these models are error-nulling models. This is equivalent to our observation that both models are based on an attractive manifold. As these models cannot explain sensitivity to action boundaries, Fajen rejects the error-nulling approach. However, we believe that may be premature. It may be possible to salvage the error-nulling approach by introducing a level of parameter dynamics (Saltzman & Munhall, 1992). Specifically, the stiffness parameter $b$ need not be fixed, but may vary according to information-based dynamics. If not only pseudoattractor location but also pseudoattractor strength is modulated on the basis of incoming information, it may be possible that sensitivity to action boundaries can be demonstrated within the information-based, error-nulling framework.

In what follows, we use the deceleration-error model as a base, and introduce new elements in order to meet the demands of affordance-based control (Fajen, 2005a, 2007a) within the modeling tradition of information-based control and behavioral dynamics (Warren, 2006).

## Modeling Affordance-Based Control

We now turn to the question of how to capture the flexibility allowed by affordance-based control with modulations of the stiffness parameter. The control law should enforce a hard constraint, ensuring that braking before collisions remains possible at all times, while also allowing for an influence of soft constraints, such as being in a hurry. A reasonable starting point is to assume that the relative importance of these constraints depends on the actor's proximity to the action boundary, beyond which a collision is inevitable. When the actor is relatively far from the obstacle, he or she may be far from the action boundary. In this situation, soft constraints should have a greater influence on behavior, as the need to brake is not urgent. With an obstacle in the distance, the actor is likely to maintain cruising speed, particularly if the actor is in a hurry. As the actor approaches the obstacle, the proximity to the action boundary also decreases and the urgency of braking becomes greater. This corresponds with an increase in the relative strength of the hard constraint. At some point, as the action boundary is reached, the hard constraint should become the only consideration, outweighing all soft constraints. For example, in an emergency braking situation, a cautious driver and an aggressive driver should both brake at full strength.

From this sketch, the desired modulation of the pseudoattractor strength begins to emerge. As the action boundary is approached, the pseudoattractor strength should increase. At the action boundary, the strength should become infinite, outweighing the influence of other constraints. This has the effect of allowing a trade-off between hard and soft constraints away from the action boundary, while also ensuring that the hard constraint becomes the only consideration near the boundary. Under this strategy, the hard constraint for braking demarcates state space at the affordance boundary, defining the set of possible trajectories that result in successful braking. The collapse of the possible into the actual is delegated to the soft constraints, opening up new modeling questions, such as how aggressive driving can be represented dynamically as a soft constraint.

With these considerations, we propose that the strength of the pseudoattractor should be inversely proportional to the proximity to the action boundary. Key here is the realization that "proximity" need only be loosely defined. The only requirement for approximate action-boundary proximity is that it is a smooth function with a value of zero at the action boundary, and greater than zero otherwise. If we define the action boundary to be at $a_{\text{ideal}} = a_{\text{min}}$, given some constant maximum achievable deceleration $a_{\text{min}}$, one possibility is

$$p(\boldsymbol{\alpha}) = \frac{a_{\text{ideal}} - a_{\text{min}}}{a_{\text{min}}}, \tag{9}$$

where $p(\boldsymbol{\alpha})$ is the approximate action-boundary proximity. Under Equation 9, $p(\boldsymbol{\alpha}) = 0$ when $a_{\text{ideal}} = a_{\text{min}}$, and $p(\boldsymbol{\alpha}) > 0$ when $a_{\text{ideal}} > a_{\text{min}}$. As $a_{\text{ideal}}$ approaches $a_{\text{min}}$, $p(\boldsymbol{\alpha})$ will approach zero.

Thus, allowing stiffness to vary inversely with approximate action-boundary proximity, we propose a new model of visually guided braking:

$$\dot{a} = \Psi_3(\boldsymbol{\alpha}) = -b'_a\left(\frac{a_{\text{min}}}{a_{\text{ideal}} - a_{\text{min}}}\right)(a - a_{\text{ideal}}). \tag{10}$$

## Calibration

For this model to be plausible, we must demonstrate that maximum deceleration $a_{\text{min}}$ is available to actors in the course of braking. This is a challenge, as it seems impossible that $a_{\text{min}}$ could be specified optically, as it is a function of the action system's mechanics rather than an actor–environment relation. The answer is that there are higher order invariants, contingencies between actions and perceptual consequences, that are specific to $a_{\text{min}}$. These contingencies can be discovered through a process of calibration. Fajen (Bastin, Fajen, & Montagne, 2015; Fajen, 2005a, 2005b, 2005c, 2007a, 2007b, 2008b) has developed a convincing case for this possibility on the basis of theoretical considerations as well as empirical results.

To begin with the latter, there is evidence that drivers are sensitive to maximum brake strength. Fajen (2005c) observed that when brake strength is manipulated between participants, the ratio $a_{\text{ideal}}/a_{\text{min}}$ is invariant across groups (Fajen, 2005c). This dimensionless, action-scaled ratio echoes the findings of body-scaled $\pi$ numbers found in classic studies of affordance perception (Mark, 1987; Warren, 1984). Furthermore, within-subject manipulation of brake strength revealed partial trial-to-trial recalibration, suggesting a relatively fast calibration process. In another study, Fajen (2007b) demonstrated that complete recalibration to changes in brake strength can occur within a single block of 15 trials. A follow-up experiment investigated the contribution to recalibration of information about the trial outcome (whether a collision was successfully avoided) by blacking out the driving-simulator screen 1 s after brake onset. Calibration was achieved as before, indicating that the optical consequences of the brake adjustment, rather than final trial outcome, were responsible for recalibration. Recalibration has also been demonstrated in an interception task, in which the experimental intervention to action capabilities was in terms of maximum speed rather than maximum achievable deceleration (Bastin et al., 2010). Together, these studies establish that actors respond appropriately to changes in action boundaries.

The remaining question is how action boundaries are perceived. Recall from Equation 7 that $a_{\text{ideal}}$ is specified by optical variables. This higher order variable has units of distance over time-squared. It is implausible that $a_{\text{ideal}}$ is perceived in the arbitrary, extrinsic units of meters and seconds. Although an intrinsic unit exists for distance (eyeheight), there is no equivalent for time. The alternative is that observers detect information about $a_{\text{ideal}}$ in units of $a_{\text{min}}$ (Fajen, 2005a, 2005c). This would obviate the need to determine the ratio $a_{\text{ideal}}/a_{\text{min}}$ after independently detecting each variable. Calibration is then the process of adjusting the metric in which $a_{\text{ideal}}$ is measured on the basis of experience.

The perceptual consequences of braking adjustments may allow the actor to arrive upon an accurate metric even in the absence of specific optical information (Fajen, 2005c). If pedal position can be perceived in units of maximum pedal depression, this information can be the basis for calibration. When the actor is correctly calibrated, and the pedal position matches $a_{\text{ideal}}$ in units of $a_{\text{min}}$, then $a_{\text{ideal}}$ will stay constant. However, if the actor is not calibrated, then perceived ideal deceleration will drift away from the current brake position. This phenomenon corresponds to the situation in which driving conditions change, and a brake position that would have previously been adequate is no longer enough to prevent a collision. In this situation, the perceived urgency of deceleration continues to increase even after the onset of braking. The intuitive response is to increase the brake strength. When the perceived urgency of deceleration is no longer drifting dangerously upward, the correct metric has been reacquired.

If this is possible, then the fraction $a_{\text{ideal}}/a_{\text{min}}$ in Equation 10 is indeed available to the actor, on the basis of contingencies between braking and perceptual outcome. However, we also note that $a_{\text{ideal}}$ also appears elsewhere in the model. Given the previous discussion of calibration, one might argue that this also be scaled by $a_{\min}$. The same argument can be made for current deceleration $a$. Therefore, we reinterpret Equation 10 by scaling the entire parenthetical ($a - a_{\text{ideal}}$) by $a_{\min}$. This can be done without affecting model behavior by substituting $b'_a = b_a / a_{\min}$ into Equation 10. Thus, we introduce a new stiffness parameter $b_a = b'_a a_{\min}$. This leaves us with

$$\dot{a} = \Psi_3(\boldsymbol{\alpha}) = -b_a\left(\frac{a_{\min}}{a_{\text{ideal}} - a_{\min}}\right)\left(\frac{a - a_{\text{ideal}}}{a_{\min}}\right), \tag{11}$$

which we can then simplify to

$$\dot{a} = \Psi_3(\boldsymbol{\alpha}) = -b_a\left(\frac{a - a_{\text{ideal}}}{a_{\text{ideal}} - a_{\min}}\right). \tag{12}$$

The fraction in Equation 12 captures the intuitions we have developed regarding visually guided braking. The numerator defines the pseudoattractor location, ensuring that no further adjustments are required when $\dot{\tau} = -0.5$. The denominator then defines (inversely) the pseudoattractor strength, going to zero as the action boundary is approached. This corresponds to the perception of urgency to decelerate, allowing it to be defined not only by deviation from $\dot{\tau} = -0.5$ but also by proximity to the action boundary.

## Soft Constraints

Equation 12 describes how the hard constraint of the action boundary might be modeled dynamically. The question of soft constraints has yet to be addressed.

Recall the earlier discussion about flexibility: Affordance-based control relaxes the control law, such that it describes a broad necessary condition for success rather than a specific sufficient condition for success. In other words, affordance-based control allows for multiple successful trajectories for the same situation. It cannot be the control law itself that determines which trajectory is ultimately realized. It is only from interaction between the control law and soft constraints that possibility is collapsed into actuality. Thus, simulations of Equation 12 on its own would be of little interest. Rather, soft constraints should be introduced to the dynamics.

Soft constraints have not previously been studied in the context of behavioral dynamics. Perhaps this is because it is usually impossible to combine control laws with other dynamical terms without compromising the control law. For example, if another term were introduced in Equation 8, its nullcline would shift away from $\dot{\tau} = -0.5$. As a result, such a model may result in a collision at every simulation. As a result of similar considerations, many control laws from the perception-action literature can only be modeled by themselves. Any additional terms would result in a loss of the desired phenomenology.

The approach we have outlined allows us to circumvent this limitation. To demonstrate, we introduce a naive soft constraint that nominally models an actor's desire to maintain a comfortable speed. We also consider variations in this preference. Perhaps aggressive drivers prefer to maintain their speed over most other considerations, whereas cautious drivers decelerate more readily. This preferred-speed constraint can be modeled as

$$\dot{a} = \Psi(\boldsymbol{\alpha}) = -b_v(v - v_{\text{p}}), \tag{13}$$

where $b_v > 0$ is a stiffness parameter defining the strength of the preference, and $v_{\text{p}}$ is the actor's preferred speed. Thus, when $v < v_{\text{p}}$, the actor will be influenced to accelerate (or reduce deceleration). We do not necessarily think that Equation 13 is an accurate model of driving styles, but it should suffice as a foil against which to test Equation 12.

Combining Equation 12 and 13, we arrive at

$$\dot{a} = \Psi(\boldsymbol{\alpha}) = -b_v(v - v_{\text{p}}) - b_a\left(\frac{a - a_{\text{ideal}}}{a_{\text{ideal}} - a_{\min}}\right). \tag{14}$$

## Numerical Results

As a proof of concept, we tested the effect of different "styles of control" by varying the parameter $b_v$ in Equation 14. Low values of $b_v$ correspond to cautious drivers who place a relatively high importance on collision avoidance; high values of $b_v$ correspond to aggressive drivers who place a relatively high importance on maintaining a fast speed. Appendix B includes the details on the numeric methods we employed.

Figure 3 shows the resulting trajectories for low, medium, and high values of $b_v$, the strength of the preferred-speed soft constraint. All other parameters were held constant. The simulations are characterized by an initial braking followed by a coasting period of small, constant deceleration. Eventually, an increase in deceleration is observed as the obstacle is approached.

The simulation with low $b_v$, corresponding to a weak speed preference, comes closest to the previous simulations of the $\dot{\tau}$ and deceleration-error control laws. The initial deceleration nearly reaches the ideal deceleration producing $\dot{\tau} = -0.5$, and $\dot{\tau}$ never drops below $-0.7$ during the coasting period. Despite the relatively cautious approach, a drastic increase in deceleration is observed at the end of the trial.

The high value of $b_v$ represents a more aggressive driver, reluctant to brake except when absolutely required to avoid a collision. In this case, some deceleration is nevertheless observed at simulation onset; however, a speed near to $v_{\text{p}}$ is stabilized. This speed is maintained until braking becomes necessary. When this occurs, maximum deceleration is attained rapidly.

These simulation results show the possibility of incorporating sensitivity to action boundaries into existing control laws. Additionally, they demonstrate the different roles of hard and soft constraints. A hard constraint defines the behavior's conditions for success: satisfaction of the control law without violation of the action boundary. One or more soft constraints influence the specific trajectory of the system within the safe region defined by the hard constraint.

Despite its apparent plausibility, the simulated behavior depicted in Figure 3 is unrealistic in at least one respect. Specifically, for the majority of the simulations, $\dot{\tau} < -0.5$, with the exception of the final moments when $\dot{\tau}$ reaches the margin value. Equivalently, deceleration remains below what is required until a collision becomes imminent. At no point does the simulated actor brake more than is required, producing $\dot{\tau} > -0.5$. This contradicts observations of both humans (Fajen, 2005a, 2005c; Yilmaz & Warren, 1995) and hummingbirds (Lee et al., 1991), both of which frequently overshoot $\dot{\tau} = -0.5$.

To reconcile these observations with the modeling strategy proposed here, consider the two types of terms we have modeled: hard and soft constraints. The hard-constraint term, characterized in Equation 14 by the deceleration-error control law, could explain excessive braking by a change in the nullcline location. Instead of defining ideal acceleration $a_{\text{ideal}}$ as the acceleration that produces $\dot{\tau} = -0.5$, it could be defined as acceleration that produces $\dot{\tau} = -0.45$ or any other value greater than $-0.5$. Alternatively, the nullcline could be located at some constant offset from $a_{\text{ideal}}$. This could be justified by noting that the consequences of braking excessively are minor, whereas braking too little could potentially be catastrophic. Thus, it would make sense for some margin for error to be built in to the control law.

Nevertheless, this is an unsatisfying solution. The sample trials depicted in previous experiments (Fajen, 2005c; Yilmaz & Warren, 1995) do not appear consistent with the hypothesis that participants were attracted to some nullcline defined either in terms of $\dot{\tau} > -0.5$ or $a < a_{\text{ideal}}$, although this has not been specifically tested. Whatever the location of the nullcline, it could be wondered whether our model captures the full flexibility of perceptually guided action, including the potential of the behavioral system to occupy states on either side of the nullcline.

If not explained by the location of the attractive nullcline, perhaps excessive braking could be captured with soft constraints. Soft constraints characterize not the conditions of success or failure of the action but rather a style of control or manner of acting. Decelerating minimally and decelerating excessively are two styles of control that are both compatible with the hard constraint of avoiding a hard collision. The soft constraint introduced in Equation 13, representing a preferred speed, influences the actor to accelerate as a stop is reached. Thus, it illustrates that the hard constraint is not violated by a soft constraint working in the opposite direction. However, it may now be instructive to examine a soft constraint that works in the same direction as the hard constraint. That is, we will test whether the addition of a soft constraint promoting deceleration in the final moments of the trial can result in excessive deceleration.

To that end, we consider that the actor may have not only a preferred speed but also a preferred distance from the obstacle. If the actor is further than this distance, all else equal, he is likely to accelerate. If the actor is closer than this distance, all else equal, he is likely to decelerate. Thus, we consider the addition of a simple nullcline

$$\dot{a} = \Psi(\boldsymbol{\alpha}) = -b_d(x + d_{\text{p}}), \tag{15}$$

where $b_d > 0$ is a stiffness parameter and $d_{\text{p}}$ is the actor's preferred distance. Note that this soft constraint, representing a preference for $x = -d_{\text{p}}$, comes into direct conflict with the hard constraint, representing the necessity of $x = 0$. Thus, we should predict that this preferred-distance constraint will not be satisfied. Nevertheless, the additional term may demonstrate that the hard constraint does not preclude excessive braking. We combine Equation 14 with Equation 15 to arrive at a model including a hard constraint for braking, a preferred-speed soft constraint, and a preferred-distance soft constraint, as follows:

$$\dot{a} = \Psi(\boldsymbol{\alpha}) = -b_d(x + d_{\text{p}}) - b_v(v - v_{\text{p}}) - b_a\left(\frac{a - a_{\text{ideal}}}{a_{\text{ideal}} - a_{\text{min}}}\right). \tag{16}$$

Figure 4 shows the results of these simulations. All details, including the three values of the preferred-speed stiffness $b_v$, were the same as in Figure 3. Notably, excessive braking such that $\dot{\tau} > -0.5$ is observed in the $b_v = 0.1\ \text{s}^{-2}$ simulation. Thus, these simulations demonstrate that the hard constraint for braking is compatible with styles of control that place the system state on either side of the hard-constraint nullcline.

This preferred-distance constraint, like the preferred-speed constraint, is ad hoc and intended only for illustration. Indeed, the purported preference for a certain distance is not evident in the simulations. However, by demonstrating the possibility of combining control laws with other model terms, we have made it possible for researchers to give the same attention to soft constraints that they have given to the control laws themselves. This should result in the discovery of soft constraints that more closely match observed behavior. The present point is merely that the hard constraint ensures completion of the task. The specific manner in which the task is completed, corresponding to the flexibility of visually guided action, is determined by any number of soft constraints.

## Recommendations for the General Case

The approach that we have used to model the effect of action boundaries on the control of soft collisions can also be applied in the context of other visually guided behaviors. To that end, in this section, we will describe the modeling strategy in general terms.

We divide the process of modeling affordance-based control laws into three broad stages. At each stage, the modeler will encounter alternative possibilities for proceeding. These choice points provide opportunities for experimentation to resolve competing modeling decisions.

### Behavioral Dynamics

The first stage is to model the underlying control law. Here, we recommend an approach based on behavioral dynamics (Warren, 2006), with some previously discussed modifications. The modeler should first identify the state space of the animal–environment system with a vector of state-space variables $\boldsymbol{\alpha}$. A control law should be developed in the form of Equation 2, $\dot{\boldsymbol{\alpha}} = \boldsymbol{\Psi}(\boldsymbol{\alpha}, \mathbf{i})$. The control law represents the system's intrinsic dynamics modulated by information $\mathbf{i}$. The information variables should themselves be a function of the system state, in the form of $\mathbf{i} = \boldsymbol{\lambda}(\boldsymbol{\alpha})$.

We have not addressed whether it is permissible to have state variables $\boldsymbol{\alpha}$ in the control law rather than a description solely in terms of informational variables $\mathbf{i}$. This issue is closely tied to the role of intrinsic dynamics within the control law. Our intuition is that the intrinsic dynamics should be described in terms of state variables, whereas the actor's modulation of the intrinsic dynamics should be based only on available information. To our knowledge, there is no general method of mathematically distinguishing these aspects of a control law. This is an area in which further development of the behavioral dynamics formalism is warranted.

In any case, the control law should determine an attractive nullcline $\boldsymbol{\Psi}(\boldsymbol{\alpha}, \mathbf{i}) = \mathbf{0}$. The nullcline determines the system's gross behavior and is the primary consideration when developing a control law. One strategy is to first find a nullcline and then test various control laws that are consistent with it. This is what we have done here, comparing two control laws that create the nullcline $\dot{\tau} = -0.5$. In this case, the control laws resulted in similar patterns of behavior (see Figure 1), consistent with our view that the nullcline is of primary importance.

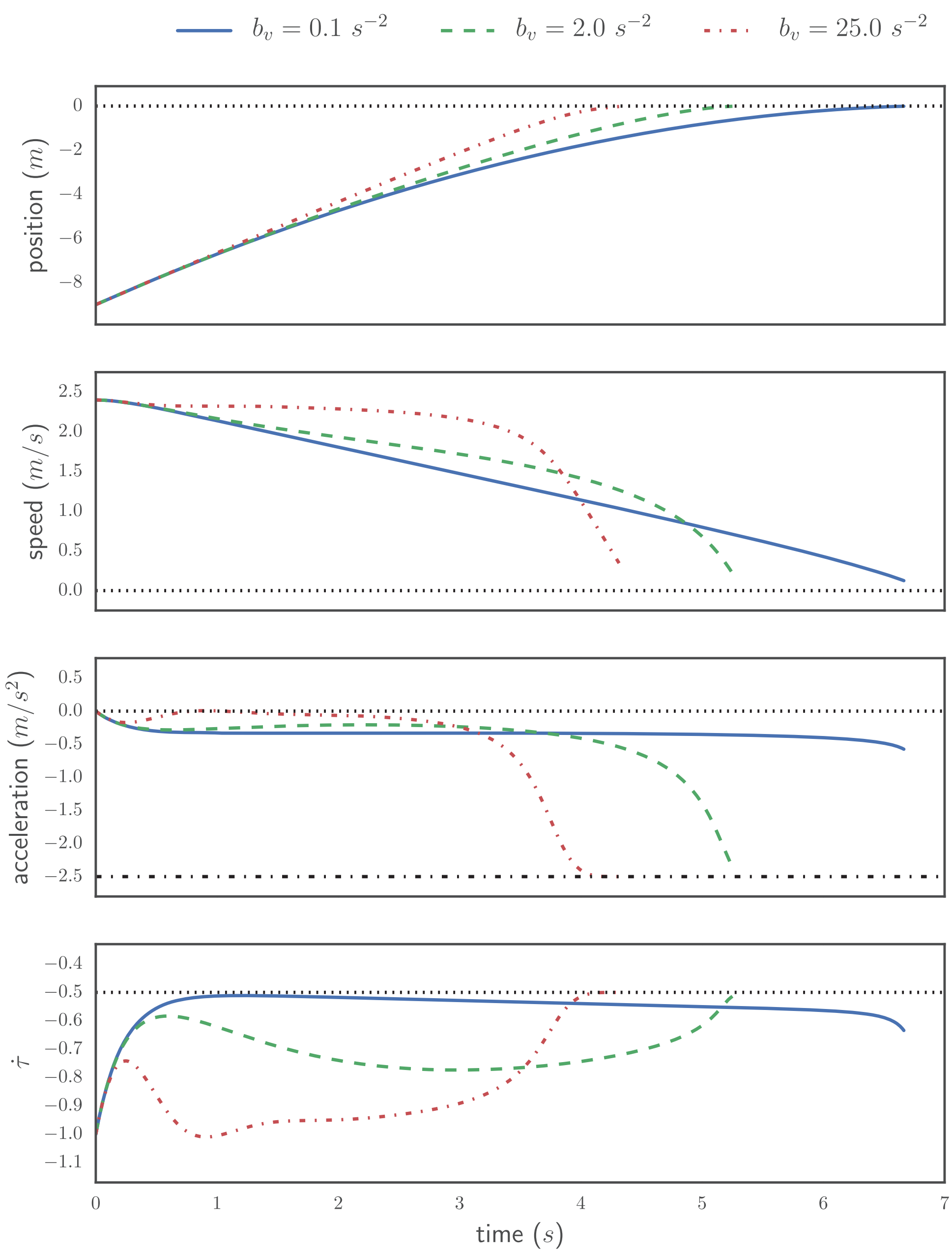


*Figure 3.* Solutions of Equation 14, for three values of $b_v$, with $b_a$ = 10 m/s$^3$, $a_{\mathrm{min}}$ = – 2.5 m/s$^2$ (represented by the dash-dotted line in the plot of $a$), and $v_{\mathrm{p}}$ = 2.4 m/s, estimated using the lsoda solver in the FORTRAN library odepack (Hindmarsh, 1983), with a maximum step time of $h$ = 0.0001 s. Appendix B provides a discussion about the accuracy of these estimates. See the online article for the color version of this figure.

## Affordance-Based Control

The second stage of the process is to introduce further modulation of the control law such that action boundaries are respected. To this end, the relevant action boundary should be identified with a manifold in state space separating physically possible states from physically impossible states. Then, a proximity function $p(\boldsymbol{\alpha})$ should be developed. The proximity function must satisfy $p(\boldsymbol{\alpha}) = 0$ on the action-boundary manifold and $p(\boldsymbol{\alpha}) > 0$ within the allowed region, and vary smoothly across state space.

The control law is then modified by varying $\dot{\boldsymbol{\alpha}}$ in inverse proportion to the proximity function. That is, the previous control law should be divided by the proximity function. This modulation turns the control law into a hard constraint, ensuring that it is satisfied before the action boundary is violated. Thus, the control law now describes not only sufficient but also necessary conditions for successful action.

The resulting term can then be simplified, with information variables substituted for state variables when appropriate. This simplification is likely to provide testable insights about action-scaled per-

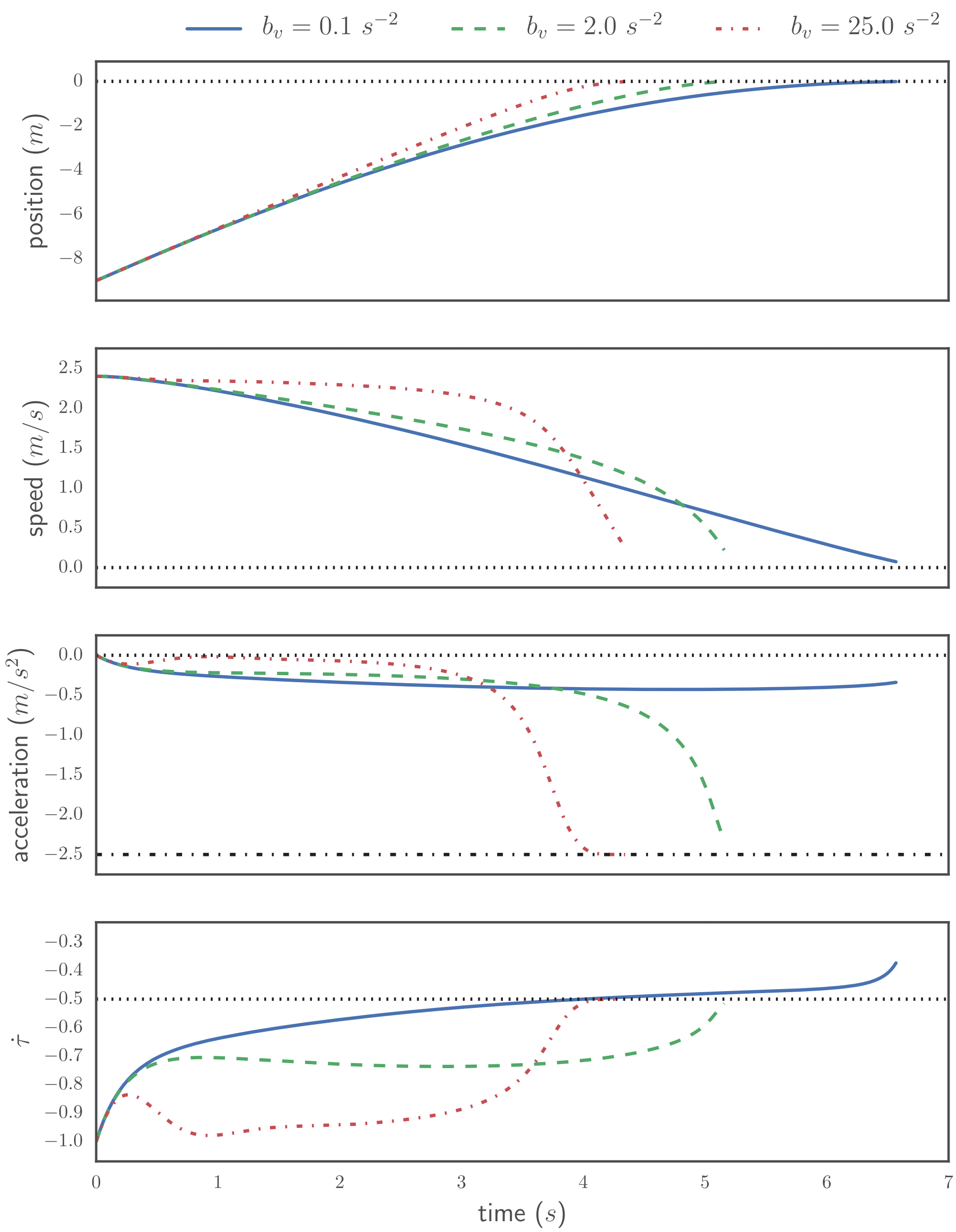


*Figure 4.* Solutions of Equation 16, for three values of $b_v$, with $b_d$ = 0.1 $s^{-3}$ and $d_p$ = 3.0 m. All other parameters and simulation details are the same as in Figure 3. See the online article for the color version of this figure.



ception and calibration. For example, in the model we developed here, we arrived at the quotient $a_{\text{ideal}}/a_{\text{min}}$, echoing Fajen's (2005a, 2005c) proposal for braking calibration, according to which $a_{\text{ideal}}$ is perceived in units of $a_{\text{min}}$.

## Soft Constraints

The third stage of the modeling process is to explore soft constraints that influence behavior but do not define success or failure. This type of inquiry is necessary to understand why a specific trajectory is taken through the safe region, but it has rarely been undertaken. Without modulation by a proximity function, the combination of a soft constraint with a control law is likely to result in unsuccessful action. Thus, until now, it has been difficult to include soft constraints in behavioral dynamics.

However, soft constraints need not be mysterious. The methodology we used to develop two prototypical soft constraints, preferred speed and preferred distance, is similar to the process of developing control laws. That is, we focused primarily on the nullcline defining a desired state of affairs. Indeed, the only difference between hard and soft constraints is that the former are parameterized using a proximity function. In the final model, the hard constraint and any number of soft constraints are summed, each constraint corresponding to one term, to produce the rate of change of the state variables.

The soft constraints we introduced here are meant as proofs of concept rather than specific predictions of behavior. In the future, the same care should be taken in modeling soft constraints, as has been applied in the past to control laws. A similar investigation of state space can be undertaken as for control laws, focusing on nullclines, pseudoattractors, and pseudorepellers. Additionally, the variables used in the modeling of soft constraints should be available to the actor in local arrays of structured energy distributions.

Of course, the validity of soft constraints should be experimentally confirmed. To that end, the resulting model of the behavioral dynamics, including both hard and soft constraints, can generate testable predictions. For example, although our preferred-distance soft constraint was empirically motivated (by the observation that actors overshoot $\dot{\tau} = -0.5$), it was not compared with alternative soft constraints that would produce the same gross behavior. Further investigation would use behavioral dynamics models to find conditions for which hypothetical soft constraints make different predictions. Then, an experiment could be designed that would disambiguate between them accordingly.

## General Discussion

We have shown that affordance-based control (Fajen, 2007a) can be understood as a refinement of information-based control (Warren, 2006) rather than a completely novel approach to visually guided action. We have described a method for expanding the scope of control laws from a description of sufficient conditions for successful action to a description of necessary conditions. This allows us to understand action as not only control of actuality but also control of possibility.

This shift in theoretical perspective motivates two related changes in the dynamical description of visually guided action. First, we dynamically adjust the strength of the control law's pseudoattractor on the basis of ongoing optical information, such that pseudoattractor strength goes to infinity in the limit as the action boundary is reached. As a result, the action boundary becomes a hard constraint that is impossible to violate. Second, we add to the control-law term additional terms representing soft constraints on perceptually guided action, such as contextual factors. Only in the interaction between the soft and hard constraints can the dynamics of affordance-based control be observed.

### Empirical Investigation

To demonstrate the plausibility of our modeling approach, we have developed a dynamical model of visually guided braking. Our model is firmly grounded in existing braking-control laws (Fajen, 2005a; Lee, 1976; Warren, 2006) and it also adheres to the principles of affordance-based control (Fajen, 2007a). However, we have not subjected the proposed models to an empirical investigation. In part, this is because we are formalizing existing proposals, so much of the experimental work has already been done. The many experiments of Fajen (2005a, 2005c, 2008a, 2008b) that we have reviewed, for example, make a convincing empirical case for affordance-based control. Furthermore, as Equations 14 and 16 are intended only as proofs of concept, we are not interested in testing them specifically.

Instead, the best test of our framework will be its use to guide questions about soft constraints. In general, the premise that could be tested is that actors will show systematic differences in their behavior when soft constraints are manipulated experimentally, even if they use the same control law. For example, one might vary the context in which participants perform visually guided braking, with some participants in a racing scenario and others in a safety test.

It should not be surprising that this kind of manipulation would cause differences in performance. Nevertheless, the union between affordance-based control and behavioral dynamics allows us to make some basic predictions. First, we should be able to characterize both groups' trajectories as consistent with the same control law, despite the differences between them. This can be examined not only on the basis of model fit but also by surreptitiously manipulating optical information (as in Fajen, 2005a, Fink et al., 2009, and Warren et al., 2001, for several examples).

Second, the differences between the groups should be systematic, reflecting the soft constraints implied by the instructions. Hypothesized soft constraints can be tested against one another on the basis of model fit, as well as by manipulating implicated variables. In general, we should be able to experimentally manipulate the specific trajectory taken by a participant without affecting the optical information they are using.

Finally, we can make predictions as to the impact of adjusting participants' action boundaries. For example, decreasing the size of the safe region should reduce the variation caused by differences in soft constraints.

Of course, more specific predictions can be made on the basis of the scaling relationships evident in a specific dynamical model. For example, Equation 14 involves a scaling of ideal deceleration by maximum deceleration, the same scaling relationship proposed by Fajen (2005a, 2005c). Fajen (2005c) manipulated brake strength in a virtual driving task, observing recalibration consistent with this scaling relationship. Other models of affordance-based control may implicate other scaling relationships, which can then be tested analogously.

As our approach is derivative of information-based and affordance-based control, it is not surprising that the investigation of its models would employ similar experimental techniques as those two previous perspectives on visually guided action. In general, empirical studies using our approach will be familiar to anyone using modeling to guide experimental inquiry. Hypotheses can be formulated in terms of the model components and evaluated on the basis of model fit.

### The Error-Nulling Assumption

Our model may seem to depart from affordance-based control in one major respect. Central to Fajen's approach is the rejection of what he terms "the error-nulling assumption" (Fajen, 2005b). The error-nulling assumption is the dynamical strategy of developing a model around a nullcline that represents a desired state of affairs for the actor. This is, of course, exactly what we have done, inspired by the framework of behavioral dynamics (Warren, 2006). Thus, one could argue that by embracing error-nulling, we have not modeled affordance-based control at all. However, our analysis of the braking problem revealed that affordance-based control is not necessarily incompatible with the error-nulling assumption. The consideration of action boundaries contextualizes the process of error-nulling rather than replacing it.

This is not merely a watering down of Fajen's (2005b) position. He argues that sometimes an adjustment is necessary, and other times it is not, depending on the proximity of the actor to an action boundary (p. 726). The question then becomes whether to characterize this adjustment as error-nulling or as something else. Fajen proposes that actors are not relaxing to some ideal state, but rather they are keeping the ideal state within the safe region (equivalently, avoiding the action boundary). He notes that actors behaving in such a way would appear to be nulling an error even though they are doing something else.

This phenomenological similarity between error-nulling and affordance-based control is a key point. If both models make similar predictions, adjudicating between them may prove difficult. Are actors moving toward the ideal state, or away from the action boundary?

However, the resolution to this impasse is deceptively simple: These alternatives are in fact equivalent. As long as the action boundary is defined with reference to the ideal state, then avoiding the action boundary necessitates moving toward the ideal state, and vice versa. Avoiding the action boundary, then, is *conditional* error-nulling; it is error-nulling prioritized by proximity to the action boundary. Thus, avoiding the action boundary need not be an entirely novel control strategy. Rather, it may be a modulation of the error-nulling strategy whereby the urgency of nulling the error depends on the action boundary. This modulation allows for situations wherein the actor's behavior is guided primarily by the action boundary rather than the ideal state. From this perspective, our approach is faithful to affordance-based control.

In any case, it is not clear what alternatives to error-nulling are available. It is instructive to again consider the topology of dynamical-system state spaces. In dynamical terms, error-nulling is nothing more than attraction to a nullcline. Although attractive nullclines are common in information-based control models, they are not universal. For example, the control law for avoiding an obstacle by steering (Warren & Fajen, 2004) does not specify an ideal state. Rather, it specifies a state to be avoided. This control law is characterized by a repellent rather than attractive nullcline.

Most, if not all, control laws in the perception-action literature involve a single nullcline. For these models, there are only two possible topologies: attractive and repellent nullclines, or equivalently, error-nulling and error-maximizing, respectively. From a dynamical perspective, then, error-nulling is not some theory-laden assumption, but rather a basic feature of many dynamical systems. Later, we will consider the specific case of repellent nullclines in more detail.

Granted, affordance-based control does complicate this picture. It renders the nullcline more or less attractive (or perhaps, repellent), depending on circumstances. In doing so, it allows for a greater role for soft constraints. Systems with many such constraints may exhibit multiple nullclines, creating more interesting topologies. In these more complicated systems, error-nulling would be observed whenever an attractive nullcline is present. Nevertheless, a description of the system emphasizing other elements, such as action boundaries, is likely to be more explanatory than a focus on error-nulling alone.

## Perceptual Learning

Another complication to this nullcline-centric perspective concerns perceptual learning. Humans regularly acquire new perception-action abilities, each presumably involving coupling between optical (or acoustical, tactile, etc.) information and movement. The process of discovering new variables to guide action is known as *education of attention* (Jacobs & Michaels, 2007).

An illustrative example of education of attention in the realm of visually guided braking concerns the "velocity brake." Most studies of braking have used a single dynamic of the brake-vehicle system, with deceleration proportional to pedal position. Fajen (2008a) tested participants with this standard dynamic, as well as a velocity-brake condition, in which deceleration was proportional to velocity as well as pedal position. Participants did adapt to the different brake dynamics. Specifically, participants in the velocity-brake condition acted according to a different control law than participants in the normal-brake condition.

This result poses problems from the $\dot{\tau}$ theory, which does not predict any effect of brake dynamics. With the normal brake, constant deceleration (as predicted by $\dot{\tau}$) can be achieved by a constant pedal position. With the velocity, a constant pedal position entails a changing deceleration, and vice versa. Fajen (2008a) showed that participants in the velocity-brake condition used optical information consistent with a constant-pedal-position strategy rather than a constant-deceleration strategy. Therefore, the $\dot{\tau}$ strategy, and similarly the deceleration-error control law, might apply only to a specific brake dynamic.

However, these results are entirely consistent with the error-nulling approach to visually guided action. Participants in the velocity-brake condition acted according to a traditional control law, relaxing to an ideal state. Dynamically speaking, their behavior exhibited an attractive nullcline. Therefore, the modeling strategy we have outlined here could be applied to the velocity-brake control law in much the same manner as we applied it to the normal-brake control law. In general, the approach proposed here is agnostic as to which nullcline is implicated for any given perceptually guided behavior. We chose the deceleration-error control law not because we believe it to be a universal strategy for braking, but rather because of its elucidation in the existing literature. In particular, Fajen (2005a, 2005c) described his theory of calibration in terms of ideal deceleration. Our focus on the deceleration-error control law therefore allowed us to place calibration within the context of behavioral dynamics (Warren, 2006). Although our approach is not specific to the deceleration-error control law or the braking problem in general, few visually guided behaviors have received as much attention in the areas of both calibration and control.

A greater difficulty arises when we consider that control laws are learned, as the velocity-brake experiment (Fajen, 2008a) forces us to do. How do we describe behavior during the learning period? Presumably, if the actor has not yet discovered the eventual invariant, then his behavior cannot be described by the corresponding nullcline. Thus, the modeling framework we have proposed can only apply after a control law is learned. It makes no claims about the nature of perceptual learning. It therefore cannot capture the full flexibility of behavior, any more than other individual control laws can. However, it may be possible to integrate our approach with direct learning (Jacobs & Michaels, 2007). Jacobs, Vaz, and Michaels (2012) applied the direct-learning paradigm to visually guided action using control laws. The stiffness coefficient in such a model may be amenable to modulation by action boundaries in the same way we have proposed here. A simplifying assumption might be that the education of attention and sensitivity to action boundaries are orthogonal questions. Whether this is the case remains to be seen.

## Affordance-Based Control and Obstacle Avoidance

In the preceding sections, we outlined our modeling strategy in the most general terms possible. However, we must acknowledge that not all control laws take the same form as the $\dot{\tau}$ or deceleration-error strategies. It remains to be seen whether other types of control laws admit to modulation by action-boundary proximity or whether they present new difficulties for the approach.

For an example, in our discussion of the error-nulling assumption, we mentioned a control law for obstacle avoidance during locomotion (Fajen & Warren, 2003; Warren & Fajen, 2004). This control law, like its counterpart for goal-seeking during locomotion as well as the deceleration-error control law that we examined, is based on a nullcline. However, unlike the others, the nullcline for obstacle avoidance is repulsive. To prevent a collision when steering, the actor must avoid the set of states defined by the nullcline. Although we previously glossed over the distinction between attractive and repulsive nullclines, the considerations for affordance-based control are surely different.

A core concept of affordance-based control is the safe region, the area of state space within which successful action remains possible. In dynamical terms, an actor within the safe region is able to reach the (attractive) nullcline. The contribution of affordance-based control is to change the actor's admonition from "reach the nullcline, and stay there" to "remain within the safe region."

What is the safe region for a control law defined by a repulsive nullcline? One might wish to define it as the area of state space from which it is possible to avoid the nullcline. However, this definition has little explanatory force, as the entire state space (or very nearly so) would lie within the safe region. Even an actor on a collision course with an obstacle is able to change trajectory and avoid it, at any time until the last moment.

Furthermore, our analysis of the dynamics of affordance-based control relies on the fact that as the action nears completion, the safe region collapses to a point. At this point, the admonitions of information- and affordance-based control are equivalent; the only way the actor can remain in the safe region is to reach the nullcline. This ultimate equivalence provides the foundation of our reconciliation between the two approaches.

The safe region for obstacle avoidance and other repulsive nullclines does not collapse. Simply put, when reaching a goal, only one final state is satisfactory; when avoiding an obstacle, only one final state is *not* satisfactory. For this reason, modulation by action-boundary proximity is not practical for obstacle avoidance. For the same reason, though, such modulation may not be necessary. The strength of the repulsion from the obstacle-avoidance nullcline does not need to become arbitrarily high to guarantee obstacle avoidance. Even in the presence of competing constraints, finite repulsion will suffice. Therefore, action boundaries are less relevant for repulsive control laws. Without a shrinking safe region, limits on the actor's ability to move through state space will not be tested. Generalizing our approach to this class of actions may not be possible, but neither is it needed.

## Conclusions

We have introduced a modeling technique that allows us to capture the theoretical framework of affordance-based control (Fajen, 2007a) within the modeling framework of behavioral dynamics (Warren, 2006). If the strength of the attractiveness of a nullcline is allowed to vary in inverse proportion to the distance of the actor to an action boundary, then the action boundary is guaranteed to be respected. This approach not only unifies affordance-based control and behavioral dynamics but also allows for behavioral dynamics models to incorporate soft constraints without losing the nullclines that are critical to the model's phenomenology.

In the past, inquiry into visually guided action has focused on sufficient conditions for successful action. For example, following the $\dot{\tau}$-strategy will suffice to avoid a hard collision, but it is not the only way to do so. Along these lines, investigators sought to demonstrate the possibility of action guided by available information. Affordance-based control, on the other hand, emphasizes the necessary conditions for action. The actor *can* use this or that informational variable to guide action; however, the actor *must* respect its action boundaries. This perspective brought visually guided action back into contact with Gibson's (1979) theory of affordances, but it resisted the modeling success of information-based control.

In this article, we have shown that the two approaches are not mutually exclusive but rather are complementary. Information, in Gibson's (1979) ecological sense, is required for action no less under affordance-based control than under information-based control. The key concepts of affordance-based control, such as action boundaries and safe regions, correspond to dynamical entities. Behavioral dynamics provides the language in which both approaches can be compared and combined.

Using this language, we proposed a new model and reconciled the supposedly competing theories. In addition, we hope that the greatest impact of these developments will be the opening of new lines of inquiry into visually guided action. In the past, researchers have been limited to models containing a single (attractive) nullcline. We could model the dynamics of maintaining a preferred speed during locomotion, and we could model the dynamics of coming to a stop to avoid hard collision. However, we could not model both together. We were limited in understanding the flexibility and variability that humans and other animals exhibit when realizing a control law. Preferences, desires, and other factors secondary to the immediate task were little more than nuisances.

With the modeling strategy we have proposed, it is now possible to incorporate such soft constraints into the behavioral dynamics of perception and action. Our modeling of a perception-action behavior need not end with characterization of the relevant control law. Rather, we can include as many soft constraints as the situation warrants. This makes new research programs possible. We can now ask why two actors realizing the same control law might produce different trajectories. What does it mean for an aggressive driver to avoid a hard collision, in comparison with a cautious driver? How can we characterize the effects of driver distraction or intoxication? These factors are likely to influence behavior in a manner that goes beyond the choice of control law and its parametrization.

In short, we are now able to capture a wider range of the flexibility of perceptually guided action than ever before. We can now begin to study not only how perceptually guided action is possible but also how it varies between realizations and between individuals. This promises a deeper understanding of how adaptive behavior that is both stable and flexible can arise from animal–environment interactions.

## References


Andersen, G. J., & Sauer, C. W. (2004). Optical information for collision detection during deceleration. In H. Hecht & G. J. Savelsbergh (Eds.), *Time-to-contact* (Vol. 135, pp. 93–108). Amsterdam, the Netherlands: Elsevier.

Bardy, B. G., & Warren, W. H. (1997). Visual control of braking in goal-directed action and sport. *Journal of Sports Sciences, 15,* 607–620.

Bastin, J., Fajen, B., & Montagne, G. (2010). Controlling speed and direction during interception: An affordance-based approach. *Experimental Brain Research, 201,* 763–780.

Bootsma, R. J., Fayt, V., Zaal, F. T., & Laurent, M. (1997). On the information-based regulation of movement: What Wann (1996) may want to consider. *Journal of Experimental Psychology: Human Perception and Performance, 23,* 1282–1289.

Bootsma, R. J., & van Wieringen, P. C. (1988). Visual control of an attacking forehand drive in table tennis. In O. G. Meijer & K. Roth (Eds.), *Complex movement behaviour: The motor-action controversy* (Vol. 50, pp. 189–199). Amsterdam, the Netherlands: North-Holland.

Bootsma, R. J., & van Wieringen, P. C. (1990). Timing an attacking forehand drive in table tennis. *Journal of Experimental Psychology: Human Perception and Performance, 16,* 21–29.

Cavallo, V., & Laurent, M. (1988). Visual information and skill level in time-to-collision estimation. *Perception, 17,* 623–632.

Chapman, S. (1968). Catching a baseball. *American Journal of Physics, 36,* 868–870.

Fajen, B. R. (2005a). Calibration, information, and control strategies for braking to avoid a collision. *Journal of Experimental Psychology: Human Perception and Performance, 31,* 480–501.

Fajen, B. R. (2005b). Perceiving possibilities for action: On the necessity of calibration and perceptual learning for the visual guidance of action. *Perception, 34,* 717–740.

Fajen, B. R. (2005c). The scaling of information to action in visually guided braking. *Journal of Experimental Psychology: Human Perception and Performance, 31,* 1107–1123.

Fajen, B. R. (2007a). Affordance-based control of visually guided action. *Ecological Psychology, 19,* 383–410.

Fajen, B. R. (2007b). Rapid recalibration based on optic flow in visually guided action. *Experimental Brain Research, 183,* 61–74.

Fajen, B. R. (2008a). Learning novel mappings from optic flow to the control of action. *Journal of Vision, 8*(11), 12.1–12.12.

Fajen, B. R. (2008b). Perceptual learning and the visual control of braking. *Attention, Perception, & Psychophysics, 70,* 1117–1129.

Fajen, B. R., & Warren, W. H. (2003). Behavioral dynamics of steering, obstacle avoidance, and route selection. *Journal of Experimental Psychology: Human Perception and Performance, 29,* 343–362.

Fajen, B. R., & Warren, W. H. (2004). Visual guidance of intercepting a moving target on foot. *Perception, 33,* 689–716.

Fajen, B. R., & Warren, W. H. (2007). Behavioral dynamics of intercepting a moving target. *Experimental Brain Research, 180,* 303–319.

Fink, P. W., Foo, P. S., & Warren, W. H. (2009). Catching fly balls in virtual reality: A critical test of the outfielder problem. *Journal of Vision, 9*(13), 14.1–14.8.

Fitzpatrick, P., Carello, C., Schmidt, R. C., & Corey, D. (1994). Haptic and visual perception of an affordance for upright posture. *Ecological Psychology, 6,* 265–287.

Gibson, J. J. (1958). Visually controlled locomotion and visual orientation in animals. *British Journal of Psychology, 49,* 182–194.

Gibson, J. J. (1979). *The ecological approach to visual perception*. Boston: Houghton-Mifflin.

Harris, L. R., Jenkin, M. R., Zikovitz, D., Redlick, F., Jaekl, P., Jasiobedzka, U. T., . . . Allison, R. S. (2002). Simulating self-motion I: Cues for the perception of motion. *Virtual Reality, 6,* 75–85.

Hindmarsh, A. C. (1983). ODEPACK, a systematized collection of ODE solvers. In R. S. Stepleman, M. Carver, P. R. W. F. Ames, & R. Vichnevetsky (Eds.), *Scientific computing: Applications of mathematics and computing to the physical sciences* (Vol. 1, pp. 55–64). Amsterdam, the Netherlands: North-Holland.

Jacobs, D. M., & Michaels, C. F. (2006). Lateral interception I: Operative optical variables, attunement, and calibration. *Journal of Experimental Psychology: Human Perception and Performance, 32,* 443–458.

Jacobs, D. M., & Michaels, C. F. (2007). Direct learning. *Ecological Psychology, 19,* 321–349.

Jacobs, D. M., Vaz, D. V., & Michaels, C. F. (2012). The learning of visually guided action: An information-space analysis of pole balancing. *Journal of Experimental Psychology: Human Perception and Performance, 38,* 1215–1227.

Jones, E., Oliphant, T., & Peterson, P. (2001). *SciPy: Open source scientific tools for Python*. Retrieved from http://www.scipy.org/

Kaiser, M. K., & Mowafy, L. (1993). Optical specification of time-to-passage: Observers' sensitivity to global tau. *Journal of Experimental Psychology: Human Perception and Performance, 19,* 1028–1040.

Kawato, M. (1999). Internal models for motor control and trajectory planning. *Current Opinion in Neurobiology, 9,* 718–727.

Kim, N. G., Turvey, M. T., & Carello, C. (1993). Optical information about the severity of upcoming contacts. *Journal of Experimental Psychology: Human Perception and Performance, 19,* 179–193.

Kugler, P. N., & Turvey, M. T. (1987). *Information, natural law, and the self-assembly of rhythmic movement*. Hillsdale, NJ: Erlbaum.

Kugler, P. N., Turvey, M. T., Carello, C., & Shaw, R. E. (1985). The physics of controlled collisions: A reverie about locomotion. In W. H. Warren & R. E. Shaw (Eds.), *Persistence and change: Proceedings of the first international conference on event perception* (pp. 195–229). Hillsdale, NJ: Erlbaum.

Larish, J. F., & Flach, J. M. (1990). Sources of optical information useful for perception of speed of rectilinear self-motion. *Journal of Experimental Psychology: Human Perception and Performance, 16,* 295–302.

Lee, D. N. (1976). A theory of visual control of braking based on information about time-to-collision. *Perception, 5,* 437–459.

Lee, D. N. (1998). Guiding movement by coupling taus. *Ecological Psychology, 10,* 221–250.

Lee, D. N. (2014). Moving to make contact. *Ecological Psychology, 26,* 47–59.

Lee, D. N., Davies, M. N. O., Green, P. R., & van der Weel, F. R. (1993). Visual control of velocity of approach by pigeons when landing. *The Journal of Experimental Biology, 180,* 85–104.

Lee, D. N., Lishman, J. R., & Thomson, J. A. (1982). Regulation of gait in long jumping. *Journal of Experimental Psychology: Human Perception and Performance, 8,* 448–459.

Lee, D. N., & Reddish, P. E. (1981). Plummeting gannets: A paradigm of ecological optics. *Nature, 293,* 293–294.

Lee, D. N., Reddish, P. E., & Rand, D. T. (1991). Aerial docking by hummingbirds. *Naturwissenschaften, 78,* 526–527.

Lee, D. N., Simmons, J. A., Saillant, P. A., & Bouffard, F. (1995). Steering by echolocation: A paradigm of ecological acoustics. *Journal of Comparative Physiology A: Neuroethology, Sensory, Neural, and Behavioral Physiology, 176,* 347–354.

Lee, D. N., van der Weel, F. R., Hitchcock, T., Matejowsky, E., & Pettigrew, J. D. (1992). Common principle of guidance by echolocation and vision. *Journal of Comparative Physiology A: Neuroethology, Sensory, Neural, and Behavioral Physiology, 171,* 563–571.

Lee, D. N., Young, D. S., Reddish, P. E., Lough, S., & Clayton, T. M. H. (1983). Visual timing in hitting an accelerating ball. *The Quarterly*

*Journal of Experimental Psychology A: Human Experimental Psychology, 35,* 333–346.

Lopresti-Goodman, S. M., Turvey, M. T., & Frank, T. D. (2011). Behavioral dynamics of the affordance "graspable." *Attention, Perception, & Psychophysics, 73,* 1948–1965.

Lopresti-Goodman, S. M., Turvey, M. T., & Frank, T. D. (2013). Negative hysteresis in the behavioral dynamics of the affordance "graspable." *Attention, Perception, & Psychophysics, 75,* 1075–1091.

Margulis, L., & Schwartz, K. V. (1988). *Five kingdoms: An illustrated guide to the phyla of life on Earth*. New York, NY: Freeman.

Mark, L. (1987). Eyeheight-scaled information about affordances: A study of sitting and stair climbing. *Journal of Experimental Psychology: Human Perception and Performance, 13,* 361–370.

McBeath, M. K., Shaffer, D. M., & Kaiser, M. K. (1995). How baseball outfielders determine where to run to catch fly balls. *Science, 268,* 569–573.

McLeod, P., Reed, N., & Dienes, Z. (2006). The generalized optic acceleration cancellation theory of catching. *Journal of Experimental Psychology: Human Perception and Performance, 32,* 139–148.

McLeod, R. W., & Ross, H. E. (1983). Optic-flow and cognitive factors in time-to-collision estimates. *Perception, 12,* 417–423.

Michaels, C. F., & Oudejans, R. R. D. (1992). The optics and actions of catching fly balls: Zeroing out optical acceleration. *Ecological Psychology, 4,* 199–222.

Michaels, C. F., & Zaal, F. T. (2002). Catching fly balls. In S. Bennett, K. Davids, G. J. Savelsbergh, & J. van der Kamp (Eds.), *Interceptive actions in sport: information and movement* (pp. 172–183). London, United Kingdom: Routledge.

Park, H., & Turvey, M. T. (2008). Imperfect symmetry and the elementary coordination law. In A. Fuchs & V. K. Jirsa (Eds.), *Coordination: Neural, behavioral and social dynamics* (pp. 3–25). Heidelberg, Germany: Springer.

Peper, L., Bootsma, R. J., Mestre, D. R., & Bakker, F. C. (1994). Catching balls: How to get the hand to the right place at the right time. *Journal of Experimental Psychology: Human Perception and Performance, 20,* 591–612.

Pepping, G., & Grealy, M. A. (2007). *Closing the gap: The scientific writings of David N. Lee*. Mahwah, NJ: Erlbaum.

Regia-Corte, T., & Wagman, J. B. (2008). Perception of affordances for standing on an inclined surface depends on height of center of mass. *Experimental Brain Research, 191,* 25–35.

Rock, P. B., & Harris, M. G. (2006). Tau as a potential control variable for visually guided braking. *Journal of Experimental Psychology: Human Perception and Performance, 32,* 251–267.

Runeson, S. (1977). On the possibility of "smart" perceptual mechanisms. *Scandinavian Journal of Psychology, 18,* 172–179.

Saltzman, E. L., & Kelso, J. A. S. (1987). Skilled actions: A task-dynamic approach. *Psychological Review, 94,* 84–106.

Saltzman, E. L., & Munhall, K. G. (1992). Skill acquisition and development: The roles of state-, parameter-, and graph-dynamics. *Journal of Motor Behavior, 24,* 49–57.

Todd, J. T. (1981). Visual information about moving objects. *Journal of Experimental Psychology: Human Perception and Performance, 7,* 795–810.

Todorov, E. (2004). Optimality principles in sensorimotor control. *Nature Neuroscience, 79,* 907–915.

Todorov, E., & Jordan, M. I. (2002). Optimal feedback control as a theory of motor coordination. *Nature Neuroscience, 5,* 1226–1235.

Turvey, M. T. (1977). Preliminaries to a theory of action with reference to vision. In R. E. Shaw & J. D. Bransford (Eds.), *Perceiving, acting, and knowing: Toward an ecological psychology* (pp. 211–265). Hillsdale, NJ: Erlbaum.

Turvey, M. T. (1992). Affordances and prospective control: An outline of the ontology. *Ecological Psychology, 4,* 173–187.

Wann, J. P. (1996). Anticipating arrival: Is the tau margin a specious theory? *Journal of Experimental Psychology: Human Perception and Performance, 22,* 1031–1048.

Warren, W. H. (1984). Perceiving affordances: Visual guidance of stair climbing. *Journal of Experimental Psychology: Human Perception and Performance, 10,* 683–703.

Warren, W. H. (1988). Action modes and laws of control for the visual guidance of action. In O. G. Meijer & K. Roth (Eds.), *Complex movement behaviour: The motor-action controversy* (Vol. 50, pp. 339–380). Amsterdam, the Netherlands: North-Holland.

Warren, W. H. (2006). The dynamics of perception and action. *Psychological Review, 113,* 358–389.

Warren, W. H., & Fajen, B. R. (2004). Behavioral dynamics of human locomotion. *Ecological Psychology, 16,* 61–66.

Warren, W. H., & Fajen, B. R. (2008). Behavioral dynamics of visually guided locomotion. In A. Fuchs & V. J. Jirsa (Eds.), *Coordination: Neural, behavioral and social dynamics* (pp. 45–75). Heidelberg, Germany: Springer.

Warren, W. H., Kay, B. A., Zosh, W. D., Duchon, A. P., & Sahuc, S. (2001). Optic flow is used to control human walking. *Nature Neuroscience, 4,* 213–216.

Warren, W. H., Young, D. S., & Lee, D. N. (1986). Visual control of step length during running over irregular terrain. *Journal of Experimental Psychology: Human Perception and Performance, 12,* 259–265.

Wolpert, D. M. (1997). Computational approaches to motor control. *Trends in Cognitive Sciences, 1,* 209–216.

Wraga, M. (1999). The role of eye height in perceiving affordances and object dimensions. *Attention, Perception, & Psychophysics, 61,* 490–507.

Yilmaz, E. H., & Warren, W. H. (1995). Visual control of braking: A test of the tau hypothesis. *Journal of Experimental Psychology: Human Perception and Performance, 21,* 996–1014.

(*Appendices follow*)

## Appendix A

### Handling the Lack of Fixed Points in Braking Control Laws

It is tempting to treat the $\dot{\tau}$ and deceleration-error models (Equations 4 and 8) as if the actor comes to a rest at a fixed point at $(a, v, x) = (0, 0, 0)$. The error in this assumption can be seen by looking closely at Figure 1. As the simulation ends, with $v = 0$ and $x = 0$, acceleration $a < 0$ and so the actor's speed is not fixed. Thus, if the simulation were allowed to continue past this point, we would observe velocity continuing to decrease below zero, resulting in $\dot{x} < 0$ and the simulated actor moving in reverse, away from the obstacle. It is as if, by braking to a stop, the simulated vehicle subsequently goes into reverse.

This is clearly an unrealistic situation. In most vehicles, forward and reverse acceleration operate independently of each other and of the braking mechanism. One cannot go into reverse by braking hard enough. In biological locomotion, lacking easily separable mechanisms, this dichotomy is less obvious. Still, it is clear that locomoting backwards requires specific effort, distinct from the intention to come to a stop. Therefore, it is reasonable to restrict the state space of both Equations 4 and 8. Assuming we are interested in modeling only braking and not forward acceleration as well, we could revise both models with

$$a = \begin{cases} \int \dot{a}\, \mathrm{d}t, & v > 0 \\ 0, & v = 0, \end{cases} \tag{17}$$

setting deceleration to zero as soon as $v = 0$ is attained.

In physical terms, this results in a moment of infinite impulse as $v = 0$ is attained and deceleration immediately jumps to zero. This discontinuity could be seen as a drawback of the reviewed control laws. However, an in-depth comparison with the physics of stopping a moving vehicle is needed to determine the relevance of this issue. Nevertheless, this additional restriction clarifies our fixed-point analysis. Every point in the cross-section of state space defined by $v = 0$ is now a fixed-point attractor. With this revision, the system reaches stationarity as velocity reaches zero and the simulated actor comes to a complete stop.

## Appendix B

### Details of Numerical Simulations

To perform the simulations mentioned in the text, solutions of systems of ordinary differential equations were estimated using the lsoda solver in the FORTRAN library odepack (Hindmarsh, 1983), provided by the Python library SciPy (Jones, Oliphant, & Peterson, 2001).

Our strategy of making pseudoattractor strength inversely proportional to action-boundary proximity introduces a singularity in Equation 14. Specifically, the value of $\dot{a}$ is undefined at $a_{\mathrm{min}} = a_{\mathrm{ideal}}$. This can produce anomalies in numerical integration near the action boundary. The expected behavior is not always observed; this can be attributed to simulation error magnified by the singularity. The lsoda solver initially uses the Adams method for solving systems of first-order differential equations. It dynamically monitors the system's behavior, switching to the backward differentiation formula if it detects stiffness (Hindmarsh, 1983). This automatic switching is important because of the mathematical instability in Equation 14, although is not sufficient to entirely prevent anomalies. Because these errors mostly occur very close to $x = 0$, the simulations were stopped when $x \leq 0.001$ m.

(*Appendices continue*)

# Appendix C

## Dimensionality Analysis

We present here a dimensionality analysis of Equations 1 to 16 of the main text. First of all, note that the operator $[\cdot]$ yields the dimension of its argument.

Let us consider Equation 1, which reads $\tau = \theta/\dot{\theta} = -x/v$. We have $[\tau] = s$, $[\theta] =$ rad, $[x] =$ m, and $[v] =$ m/s. Consequently, the dimensionality analysis yields

$$[\tau] = \left[\frac{\theta}{\dot{\theta}}\right] = \left[-\frac{x}{v}\right] \Rightarrow s = \frac{\text{rad}}{\text{rad/s}} = s = \frac{\text{m}}{\text{m/s}} = s. \tag{18}$$

We see that all three parts of the equation exhibit consistent dimensions.

Equation 2 reads in components $\alpha_k = \Psi_k(\alpha_1, \ldots, \mathbf{i})$. We have $[\alpha_k] = V_k$ and $[\Psi_k] = V_k/s$, where $V_k$ is the respective dimension of $\alpha_k$. Consequently, left- and right-hand sides of Equation 2 have consistent dimensions.

Equation 3 reads $\Delta z = b_{\text{pedal}}(-0.52 - \dot{\tau}) + \epsilon$. We have $[z] =$ m, $b_{\text{pedal}} =$ m and $[\epsilon] =$ m. Note in this context that $[\dot{\tau}] =$ s/s $= 1$; that is, $\dot{\tau}$ is dimensionless. For Equation 3, the dimensionality analysis reads

$$\begin{aligned} [b_{\text{pedal}}(-0.52 - \dot{\tau})] &= [\epsilon] \Rightarrow \text{m} = \text{m} \\ [\Delta z] = [b_{\text{pedal}}(-0.52 - \dot{\tau}) + \epsilon] &\Rightarrow \text{m} = \text{m}. \end{aligned} \tag{19}$$

The left- and right-hand sides of Equation 3 exhibit consistent dimensions.

Equation 4 reads $\dot{x} = v, \dot{v} = a, \dot{a} = -b_{\dot{\tau}}(\dot{\tau}_m - \dot{\tau})$ with $[a] =$ m/s$^2$, $[b_{\dot{\tau}}] =$ m/s$^3$, and $[\tau_m] =$ s. Note again that $\dot{\tau}_m$ just as $\dot{\tau}$ is a dimensionless quantity. The dimensionality analysis for the first two relations is a standard exercise in classical mechanics. The dimensionality analysis for the third relation reads

$$[\dot{a}] = [b_{\dot{\tau}}(\dot{\tau}_m - \dot{\tau})] \Rightarrow \frac{\text{m}}{\text{s}^3} = \frac{\text{m}}{\text{s}^3} \cdot 1 = \frac{\text{m}}{\text{s}^3}. \tag{20}$$

Equation 5 reads $\dot{\tau} = xa/v^2 - 1$. As mentioned in the Introduction, $\dot{\tau}$ is dimensionless. Therefore, we need to check only that the first expression of the right-hand side corresponds to a dimensionless expression as well. In fact, we obtain

$$\left[\frac{xa}{v^2}\right] = \frac{\text{m} \cdot \text{m/s}^2}{\text{m}^2/\text{s}^2} = 1. \tag{21}$$

Equation 6 reads $a_{\text{ideal}} = v^2/(2x)$ with $[a_{\text{ideal}}] =$ m/s$^2$. The dimensionality analysis shows that the right-hand side exhibits in fact the same dimension as $a_{\text{ideal}}$:

$$\left[\frac{v^2}{2x}\right] = \frac{\text{m}^2/\text{s}^2}{\text{m}} = \frac{\text{m}}{\text{s}^2}. \tag{22}$$

Equation 7 reads $a_{\text{ideal}} = -k$ GOFR $/(2\tau) = -k$ ER $/(2\tau)$ with $[k] = 1$ (i.e., dimensionless), [GOFR] = [ER] = m/s. Accordingly, the dimensionality analysis for Equation 7 reads

$$[a_{\text{ideal}}] = \frac{[-k\text{GOFR}]}{[2\tau]} = \frac{[-k\text{ER}]}{[2\tau]} \Rightarrow \frac{\text{m}}{\text{s}^2} = \frac{\text{m/s}}{\text{s}} = \frac{\text{m/s}}{\text{s}} = \frac{\text{m}}{\text{s}^2}. \tag{23}$$

Equation 8 reads $\dot{x} = v, \dot{v} = a, \dot{a} = -b'_a(a - a_{\text{ideal}})$ with $[b'_a] = 1/\text{s}$. Just as for Equation 4, the dimensionality analysis needs to be carried out only for the third relation. We obtain

$$[\dot{a}] = [-b'_a] \cdot [(a - a_{\text{ideal}})] \Rightarrow \frac{\text{m}}{\text{s}^3} = \frac{1}{\text{s}} \cdot \frac{\text{m}}{\text{s}^2} = \frac{\text{m}}{\text{s}^3}. \tag{24}$$

For Equation 9, it is sufficient to note that the quantity $p$ is defined by the right-hand side of Equation 9, and consequently, the dimension of $p$ equals the dimension of the right-hand side. The right-hand side of Equation 9 is dimensionless. Therefore, $[p] = 1$.

Equation 10 is the same as Equation 8, except that the right-hand side is multiplied by the dimensionless quantity $p$. Therefore, the dimensionality analysis of Equation 10 is the same as for Equation 8.

Equations 11 and 12 are mathematically equivalent. Therefore, we only discuss Equation 12, which reads $\dot{a} = -b_a(a - a_{\text{ideal}})/(a_{\text{ideal}} - a_{\min})$ with $[b_a] =$ m/s$^3$. It is clear that the expression $(a - a_{\text{ideal}})/(a_{\text{ideal}} - a_{\min})$ on the right-hand side of the equation is dimensionless. Therefore, $b_a$ must have the same dimension as $\dot{a}$. This is the case. In fact, $b_a$ is defined as the proportionality factor or gain factor that relates the expression $(a - a_{\text{ideal}})/(a_{\text{ideal}} - a_{\min})$ to changes of $a$ given in terms of the time derivative of $a$. Therefore, the dimension of $b_a$ by definition is chosen such that the dimensionality analysis yields consistent results for the left- and right-hand sides of Equation 12.

Equation 13 reads $\dot{a} = -b_v(v - v_p)$, where $v_p$ is a velocity and has the same dimensions as $v$ (i.e., $[v_p] =$ m/s). Because $b_a$ is by definition the proportionality factor between the speed difference $(v - v_p)$ and $\dot{a}$, the dimension of $b_v$ is defined such that the dimensionality analysis yields consistent results. Explicitly, we put $[b_v] = 1/\text{s}^2$ such that

$$[\dot{a}] = [-b_v] \cdot [(v - v_p)] \Rightarrow \frac{\text{m}}{\text{s}^3} = \frac{1}{\text{s}^2} \cdot \frac{\text{m}}{\text{s}} = \frac{\text{m}}{\text{s}^3}. \tag{25}$$

From the dimensionality analyses of Equations 12 and 13 presented previously, it then follows that the two terms on the right-hand side of Equation 14 exhibit consistent dimensions and that the left- and right-hand sides of Equation 14 exhibit consistent dimensions.

Equation 15 reads $\dot{a} = -b_d(x + d_p)$, where $d_p$ is a length variable and has the same dimension as $x$ (i.e., $[d_p] =$ m). Consequently, from the dimensionality analysis, it follows that $[b_d] = 1/\text{s}^3$.

Regarding Equation 16, as with Equation 14, previous analyses show that the terms from Equations 12, 13, and 15 have the same dimensions. Thus, the dimensionality analysis for Equation 16 yields consistent dimensions for the left- and right-hand sides.

Received February 16, 2015
Revision received November 6, 2015
Accepted January 11, 2016 ■